HELSINKI INSTITUTE OF PHYSICS INTERNAL REPORT SERIES

HIP-2002-07

Cold collisions in optical lattices

Jyrki Piilo

Helsinki Institute of Physics
University of Helsinki
Helsinki, Finland

Academic dissertation
To be presented, with the permission of the Faculty of Science of the University of Helsinki, for public criticism in the Auditorium E204 of Physicum on January 9, 2003, at 10 o'clock a.m.

Helsinki 2002

ISBN 952-10-0594-7 (printed–version)
ISBN 952-10-0595-5 (PDF–version)
http://ethesis.helsinki.fi
ISSN 1455-0563
Helsinki 2002
Yliopistopaino

Preface

The work for this thesis has been done at Helsinki Institute of Physics (HIP), Theory Program, Laser Physics and Quantum Optics Project.

I am very grateful to my supervisor Prof. Kalle-Antti Suominen for sharing his knowledge of physics with me. I thank him heartfully for his support, smooth and efficient attitude during the course of work, and appreciate his good management of our research group.

HIP has provided excellent facilities to do the research for this thesis. I thank all the former and current members of our research group for numerous discussions, especially Martti Havukainen for changing ideas on the topics of computer programming, Jani Martikainen for discussions on Bose-Einstein condensate, John Calsamiglia for sharing his views on the fundamentals of quantum mechanics and quantum computing, Matt Mackie for discussions on photoassociation and for a critical reading of the introductory part of the thesis, and Emil Lundh for a collaboration on cold collisions between magnesium atoms.

I gratefully acknowledge the National Graduate School on Modern Optics and Photonics, the Academy of Finland, and the European Union IHP Research Training Network "Cold Atoms and Ultracold Atomic Clocks" for the financial support; and CSC, the Finnish IT center for science, for the computer resources. I thank my collaborator in Nordita, Kirstine Berg-Sørensen, for sharing her experience on the field of optical lattices, and for the hospitality during my visits to Copenhagen.

I have written some parts of this thesis while I have been on various locations of this globe other than Helsinki. The most precious ones for me are the two islands almost at the opposite ends of Europe: the Mediterranean Sicily, l'isola di Bella Luce e Siciliana Preferetissima, and the island of Pekka in the lake of Syvänsi, the heartlands of Finnish Savo, the location of the house of my parents Anna and Raimo. I am extremely grateful for them for trust, support, and providing me such a solid base for life. Finally, I thank my sister Maarit who taught me how to add 1 and 1, 2 and 3, and so on, while she was already attending the primary school, and I was still awaiting the moment to begin, being three years younger than her.

Helsinki, November 2002
Jyrki Piilo

Contents

Abstract

This dissertation consists of theoretical studies of dynamical interactions, specifically cold collisions, between atoms trapped in optical lattices.

The invention of laser cooling methods for neutral atoms allows optical and magnetic trapping of cold atomic clouds in the temperature regime below 1 mK. An optical lattice is a periodic structure based on matter-light interaction, and is created by polarization gradients of suitably arranged laser beams. In addition to cooling of the atomic cloud, the optical lattice traps atoms in a periodically ordered structure.

In the past, light-assisted cold collisions between atoms have been widely studied in magneto-optical atom traps. The study presented here extends the regime of cold collision research into the area of optical lattices. Cold collision studies in near-resonant optical lattices are very complicated compared to similar studies in magneto-optical traps. In the case of collisions in lattices one has to account for the internal substates of atoms, position dependent matter-light coupling, and position dependent couplings between the atoms, in addition to the spontaneous decay of atoms.

The developed quantum-mechanical model combines atomic cooling and collision dynamics in a single framework. The model is based on Monte Carlo wave-function simulations and is applied when the lattice-creating lasers have frequencies both below (red-detuned lattice) and above (blue-detuned lattice) the atomic resonance frequency.

The relevant process for red-detuned lattices is the radiative heating of colliding atoms. It is found that the radiative heating mechanism affects the dynamics of atomic cloud in a lattice in an unexpected way. Atoms, which are most mobile and energetic, are favored to participate in collisions, and are more often ejected from the lattice, than the slow ones in the laser parameter region selected for study. Thus, the atoms remaining in the lattice have a smaller average kinetic energy per atom than in the case of non-interacting atoms.

For blue-detuned lattices the efficiency of optical shielding process is studied. Complete optical shielding makes the collisions between atoms elastic, thus suppressing unwanted effects. It is found that in a blue-detuned lattice the cooling and shielding dynamics do not mix and it is possible to achieve efficient shielding process with a very simple arrangement.

The thesis is concluded with a simple study of collision rates in near-resonant lattices. The developed method allows the simplication of cold collision studies in optical lattices by combining quantum-mechanical and semiclassical models.

List of publications

This thesis consists of an introductory part, followed by four research publications.

I *Cold collisions between atoms in optical lattices*
J. Piilo, K.-A. Suominen, and K. Berg-Sørensen
Journal of Physics B: Atomic, Molecular and Optical Physics **34** (2001) L231-L237.

II *Atomic collision dynamics in optical lattices*
J. Piilo, K.-A. Suominen, and K. Berg-Sørensen
Physical Review A **65** (2002) 033411 (16 pages).

III *Optical shielding of cold collisions in blue-detuned near-resonant optical lattices*
J. Piilo and K.-A. Suominen
Physical Review A **66** (2002) 013401 (9 pages).

IV *Collision rates in near-resonant optical lattices*
J. Piilo
submitted for publication (7 pages).

Summary of publications

I A method based on Monte Carlo wave-function simulations is developed and applied for the study of cold collisions in near-resonant red-detuned optical lattices. Properties of the atomic cloud as a function of the occupation density of the lattice are calculated. The conclusion is that, for the selected laser and lattice parameter region, the colliding atoms usually escape the lattice. Moreover, the collisions selectively accelerate mainly the hotter atoms in the thermal ensemble, and thus affect the steady state which one would normally expect to reach in Sisyphus cooling without collisions.

II We give the full description of our method to study cold collisions in optical lattices, including the analytic calculations for interaction potentials, our implementation of the Monte Carlo method, and the various solutions to the computational problems. Compared to the Paper I, the results are calculated also for other atomic species, and we present a simple semiclassical analysis to support the conclusions.

III With the method developed in Papers I and II, we study the optical shielding phenomena in blue-detuned near-resonant optical lattices. The conclusion is that the cooling and shielding mechanisms can coexist in an optical lattice, and the shielding can be implemented in a simple way without the need to use laser beams other than the ones creating the lattice.

IV A simple method to calculate the collision rate between atoms in near-resonant lattices for various occupation densities of the lattice is presented. The method is based on monitoring the atomic quantum flux over the average distance between the atoms, and also brings out some new features in the Monte Carlo wave-function method when applied to cold collision problems. The developed method has a potential to simplify the study of collisions in a lattice by combining quantum-mechanical and semiclassical models.

1 Introduction

The rapid development of technology signals the ability of human beings to understand the behaviour of nature in an increasingly detailed way. Moreover, the improving human skill to control nature has led to the increasing rate of the appearance of technological applications, especially during the last one hundred years.

Better control over nature also means the ability to control and manipulate ever smaller material or electro-magnetical entities, that is, to control or manipulate nature on the single atom or single photon level. The description and control of systems on atomic scales require the use of the toolbox of quantum mechanics. This justifies the nowadays-fashionable label precision control of atoms or photons on the quantum mechanical level for many contemporary experiments, for theories developed, and for new technological solutions.

It is hard to avoid the well-advertised word nanotechnology when one reads the science pages of common newspapers recently. It remains to be seen, if the expression *precision control* breaks into the common knowledge with its association to the technological development on the edge.

Anyhow, no matter what is the reader's attitude to the recent technological developments, or to the expectations about the future technologies, it is especially true that the development of theories and methods in the field of laser cooling of a dilute gas of atoms has paved the way to the impressive and exciting developments done in theoretical and experimental physics research during the last two decades.

It has been known for a long time that light can exert a force on material objects[1]. But, it is the success of applying the light force in a controlled way to cool gaseous atomic clouds to temperatures around, and even below, the μK range which has given huge impetus to the field of cold atomic physics. In particular, the researchers working with atomic Bose-Einstein condensates have seen rapid development of their research field. Nonetheless, Bose-Einstein condensation study is not everything that can be done with cold atoms. There is a wide variety of topics ranging, e.g., from atomic cold collision studies to atomic crystal structures bound by light, optical lattices.

By now, researchers have not only learned how to cool gaseous atoms

[1]The first experiments which showed the effect of the radiation pressure of an electromagnetic field on matter predicted by Maxwell were done at the beginning of the last century [1]. It is also interesting to note that in their article [1] Nichols and Hull refer to Arrhenius who "attempts to explain the aurora borealis on similar grounds".

to temperatures near absolute zero by using laser light, but they have also learned how to trap and use these atoms for the exciting studies of the quantum physical nature of matter. This is true even on the level of single atoms. So far the emphasis has been on the fundamental research. But there are most probably only very few researchers in the cold atom physics field who doubt that important practical applications will follow in the future. The improvement of the frequency standard and consequent building of more accurate atomic clocks is an example of the influential practical applications studied with laser cooled atoms.

The work presented in this thesis falls into the category of theoretical atomic physics, and also into the field of laser cooling and trapping of atoms. The interactions between the low temperature gaseous atoms obtained by laser cooling methods are strikingly different compared ,e.g., to the atoms in room temperature. The thermal velocities of laser cooled atoms are on the scale of centimeters per second. This means that the interaction and collision dynamics of atoms occurs on a time scale that allows new kinds of phenomena to show up in the atomic interaction processes.

The study presented here concentrates on one particular laser cooling and trapping scheme, optical lattices, and on interactions between the atoms in near-resonant optical lattices. The optical lattice structure can cool atoms by the Sisyphus laser cooling mechanism [2], and finally trap atoms in an ordered lattice structure which is created by the light [3–6]. When the density of the atoms in the lattice is high enough, the interactions between the atoms begin to affect the system dynamics.

So far, most of the dynamical interaction studies between the laser cooled atoms, that is, cold collision studies, have been done for atoms in magneto-optical traps [7, 8]. The motivation for the research done in this thesis has been to extend the cold collision studies into the field of optical lattices.

The questions for which I have tried to find the answers are conceptually simple on fundamental level[2]. For example: how do the properties of the atomic cloud trapped in a near-resonant optical lattice change when the occupation density of the lattice increases so that interactions between the atoms can not be neglected? How does the outcome of the cold collisions between the atoms in the presence of a near-resonant light change when the coupling between the atoms and the trapping laser field becomes position dependent? Is the outcome of the collisions different in optical

[2]Naturally, one can not in general take for granted the conceptual simplicity when working with quantum mechanical descriptions of the systems.

lattices compared to magneto-optical traps? Do the interactions between the atoms prevent efficient cooling in optical lattices? Can optical shielding of collisions be used in an effective and simple way in blue-detuned lattices? Is it possible for the cooling and optical shielding mechanisms to coexist in the optical lattice?

The questions above are asked from either the collision or the optical lattice point of view. Thus the work presented in this thesis combines these two subfields of laser cooling: the study of cold collisions and the study of optical lattices. The questions asked are simple, but finding the answers turned out to be a very complex process. Still, it was possible to find the solutions within some simplifying assumptions and limitations.

I give here a short and simple introduction to the fields of optical lattices and cold collisions with the emphasis on the points which are necessary to understand the studies done in the included research papers. A thorough introduction into the field of laser cooling, trapping, and optical lattices can be found from a text book [9], various review articles [3–6, 10–12], and summer school lecture notes [13–16]. A detailed description of cold collision theories and experiments is given in Refs. [7, 8, 17].

The thesis is organized as follows. Chapters 2 and 3 set the temperature regimes, discuss various laser cooling techniques, and introduces red and blue-detuned lattices[3]. In Chapter 4, I describe the basic cold collision mechanisms in the presence of a near-resonant light. Chapter 5 gives our formulation of the cold collision problem in optical lattices with the central results. I conclude with a few remarks in Chapter 6.

[3]In the literature blue-detuned lattices are sometimes referred also as gray or dark optical lattices due to the reduced number of scattered photons compared to "bright" red-detuned optical lattices.

2 Temperature limits of laser cooling

Laser cooling and trapping of neutral atoms has been a very rapidly developing field of physics since the mid-eighties when experimentalists succeeded for the first time to optically trap laser cooled atoms [18]. Since then the progress of the field has featured numerous surprises and has been a fruitful combination of theory and experiments. In this Chapter I highlight some of the laser cooling mechanisms which pin down the fundamental temperature limits of laser cooling and give the temperature regime for atoms trapped in optical lattices.

Doppler cooling is based on recoil effects which damp atomic motion when an atom merely absorbs photons that propagate against its motion [9]. The photon recoil kicks an atom in a selected direction in the absorption process; but, for spontaneously emitted photons there is no preferred direction. The overall effect is the slowing of the atomic motion. This happens when two counterpropagating laser fields are detuned below, to the red side, of the atomic resonance frequency. The atom sees the photons which propagate against its motion as Doppler-shifted towards the atomic resonance and consequently prefers to absorb photons from this direction. The basic idea generalizes straightforwardly to three dimensions.

The limit of Doppler cooling in one dimension is given by the Doppler temperature

$$T_d = \hbar\Gamma/2k_B, \tag{1}$$

where $\hbar$ is Planck's constant h divided by 2π, Γ the atomic linewidth, and k_B Boltzman's constant. This limit arises due to the balance between the cooling recoil kicks against the atomic motion, and the heating effects due to fluctuations in the directions and number of the photons that the atom emits.

The theoretical description of Doppler cooling is based on a two-level model of an atom, and the semiclassical approach is typically sufficient [19]. It is possible to reach sub-Doppler temperatures by other cooling mechanisms. To understand these, the multilevel structure of an atom with various Zeeman substates in the ground- and excited-state manifolds have to be accounted for.

The first experiment, which showed that the atomic cloud can reach temperatures well below T_d, was quite puzzling for researchers [20]. Moreover, laser cooling did not seem to be as vulnerable to experimental technical errors as expected[4].

[4]For example, the slight imbalance of the intensities of Doppler cooling lasers proved

Thus, below T_d there exists another limit, the recoil limit T_r, for laser cooling [9][5]. This limit corresponds to the amount of energy of single photon absorption or emission recoil, and is given by

$$T_r = (\hbar k_r)^2 / M k_B. \tag{2}$$

Here k_r is the wavenumber of the cooling lasers, and M the mass of an atom. The corresponding recoil energy,

$$E_r = (\hbar k_r)^2 / 2M, \tag{3}$$

is the typical energy unit used in calculations.

The vicinity of T_r can be reached by the polarization gradient cooling mechanism [2,22], which is based on cooling optical pumping cycles between the various internal Zeeman substates of an atom [2]. Optical pumping of Sisyphus cooling will be explained in a more detailed way in the next Chapter.

The temperature regime of laser cooling can be lowered further since T_r does not limit the temperatures which can be achieved. The trick is that a random walk in velocity space can take an atom close to zero velocity, and thus below the recoil limit. If at this point an atom stops to absorb and emit photons, it remains trapped for a considerable time in the vicinity of the zero velocity, and consequently T_r is broken. The technique is based on the use of the dark state of an atom which is a particular superposition state. The destructive quantum-mechanical interference of excitation processes from different ground sublevels plays a key role, and the atom is prevented from being excited at all [23].

Strictly speaking this is true only for an atom that has exactly zero velocity in the laser field. With increasing interaction time between the atoms and the field, all the atoms in the cloud could reach the zero velocity region in principle. Of course, in practice the interaction time is limited, but can be long enough to allow the breaking of the recoil limit.

Hence, there exists various techniques to reach the Doppler limit T_d, and then to go below the recoil limit T_r. Some of these techniques were described above. The work presented in this thesis deals with a polarization-gradient cooling and trapping mechanism which occurs at temperatures between T_d and T_r. Sisyphus laser cooling, and the consequent trapping of atoms in

inconsequential.

[5]For typical alkaline-metal elements used for laser cooling $T_d > T_r$. Some alkaline-earth-metals have cooling transitions which have $T_d < T_r$ due to the narrow linewidths of the transitions [21].

this temperature regime, is presented in the next Chapter. A typical alkali element used for laser cooling and in the included research papers, cesium, has $T_d = 120\mu$K and $T_r = 0.2\mu$K.

The atoms in dilute laser cooled clouds interact weakly in the absence of light fields. When a light field is present, the range of interactions between the atoms increases. Moreover, when the density of the cloud is high enough, light induced inelastic collisions between the atoms begin to dominate [7, 8]. It is also possible to manipulate the interactions between the atoms by optical means, e.g., with optical shielding [8, 24, 25], which is studied in the case of optical lattices in Paper III[6].

Laser cooled atoms can be used for a great variety of purposes: 1) as a starting point for magnetic evaporative cooling to make a Bose-Einstein condensate (BEC) [11,12][7], 2) for photoassociation to produce cold molecules [8], 3) for accurate spectroscopical studies of atoms [8] 4) for studies of fundamentals of quantum mechanics [29] 5) for building of atomic clocks [10], to mention only a few examples.

[6]For atoms having extremely low nK temperatures and in the absence of light fields, magnetic fields and Feshbach resonances can be used for a manipulation of collisions between atoms [26]. See also Ref. [27] for optically induced Feshbach resonances.

[7]BEC has been created by now also by all-optical means [28].

3 Optical lattices

The Doppler cooling technique, and consequent friction-like damping of atomic motion, does not trap atoms directly. The amount of time that the atoms spend in the cooling area provided by the lasers increases with the decrease of temperature, but eventually the atoms diffuse outside the cooling region.

A necessary step from a disordered gas to ordered structures of laser cooled atoms is a periodic optical potential structure which can be created by a suitable choice of interfering laser beams [3–6, 9]. An optical lattice formed by optical potentials does not only trap the atoms, but they can also cool down via optical pumping and Sisyphus mechanism before the atoms are cold enough to localize into the optical lattice sites [2].

The analogous crystal structure in metals is created by the interactions between the atoms. In a dilute optical lattice, atoms do not interact and the lattice structure arises due to light-matter interactions. A periodic optical lattice may be realized by polarization gradients of the laser field and the consequent periodic coupling between the atoms and the laser field.

Optical lattices resemble in many respects solid-state lattices, but there exists important differences. An optical lattice is free from defects which prevent, e.g., the observation of Bloch oscillations in solid-state lattices. It is easy to control optical lattice parameters by controlling the laser field properties: lattice depth can be modified by changing the laser intensity; and the lattice can be moved by changing the polarization of the light or by chirping the laser frequency. Moreover, the optical lattice constant is typically three orders of magnitude larger than the solid-state lattice constant.

Because of the purity and ease of control in optical lattices, the atoms trapped are almost ideal for the study of lattice phenomena which are familiar from solid-state lattice studies. A few examples of these phenomena, which have been realized in experiments, include Bragg scattering [30, 31], Bloch oscillations [32], and Wannier-Stark ladders [33]. Other interesting observations include the quantum Zeno effect [34] and dynamical tunneling [35].

Modern work on optical lattices was preceded by the proposal of Letokhov to trap cold atoms in one dimension by using a standing light wave [36], and accompanied by the experiment of Burns *et al.* who created crystal structures of microscopic dielectric objects suspended in liquid by standing light waves [37]. Nowadays there exists a great variety of optical lattice designs and approaches to lattice studies. These will be explained to some extent in

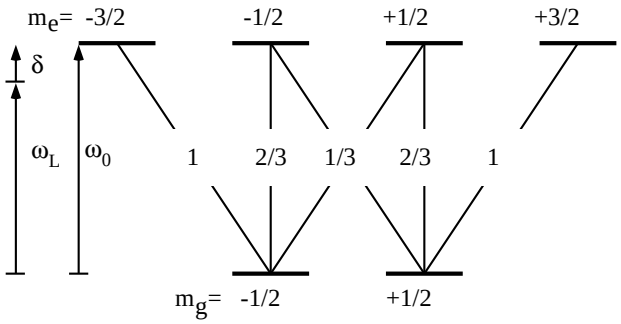

Figure 1: The level structure of a single atom for a red-detuned lattice. The squares of the Clebsch-Gordan coefficients for various transitions are shown, and the laser frequency ω_L is typically detuned few atomic linewidths below the atomic resonance frequency ω_0 for efficient Sisyphus cooling. The detuning of the laser is described by $\delta = \omega_L - \omega_0$.

the following Sections but starting with a simple one-dimensional description of Sisyphus cooling in optical lattices for both red and blue-detuned laser cases. These are the cases which we have studied. The inclusion of interactions between the atoms complicates the originally simple Sisyphus scheme but it is still possible to do a cold collision study for one-dimensional lattices.

3.1 Red-detuned optical lattices

The simplest case of Sisyphus cooling and optical lattices can be described by using the atomic level structure with the ground state angular momentum $J_g = 1/2$ and the excited state $J_e = 3/2$. A single atom has two ground state sublevels $|g_{\pm 1/2}>$ and four excited state sublevels $|e_{\pm 3/2}>$ and $|e_{\pm 1/2}>$, where the half–integer subscripts indicate the quantum number m of the angular momentum along the z direction. This is shown in Fig. 1 with the appropriate squares of the Clebsch-Gordan coefficients which describe the relative strengths of the light-induced couplings between the various levels.

This simple level structure features the necessary conditions for Sisyphus cooling in a red-detuned lattice. In a cooling optical pumping cycle, the occupied internal ground substate of an atom changes. Spontaneous emission via the excited state takes the atomic population into previously unoccupied ground state Zeeman sublevel, so that more than one ground substate is required for cooling. Moreover, the light shifts lower the energy

of the ground state sublevels when a red-detuned light is used. Thus, in a dissipative environment atoms become trapped around the points in space where the atom-laser interaction has its maximum value. For trapping in a lattice site this means that the strongest transition for the particular ground substate should not lead to optical pumping out of the trapping level at the middle point of a lattice site. This is avoided when the angular momentum of the excited state is larger than for the ground state, and when the coupling between the stretched ground and excited sublevels gives the largest light shift contribution.

3.1.1 Sisyphus cooling

The laser field consists of two counter–propagating beams along the z-axis with orthogonal linear polarizations and with frequency ω_L. The total field has a polarization gradient in one dimension and reads (with suitable choices of phases of the beams and origin of the coordinate system)

$$\mathbf{E}(z,t) = \mathcal{E}_0(\mathbf{e}_x e^{ik_r z} - i\mathbf{e}_y e^{-ik_r z})e^{-i\omega_L t} + c.c., \tag{4}$$

where $\mathcal{E}_0$ is the amplitude and k_r the wavenumber. With this field, the polarization changes from circular σ^- to linear and back to circular in the opposite direction σ^+ when z changes by $\lambda_L/4$ where λ_L is the wavelength of the lasers. See Fig. 2 for the points of pure circular polarization with the corresponding lattice wells.

The periodic polarization gradient of the laser field is reflected in the periodic light shifts, i.e., AC–Stark shifts, of the atomic sublevels creating the optical lattice structure. The relative strengths of the couplings between a single ground state sublevel and various excited state sublevels vary spatially according to the polarization of the light field due to unequal values of the Clebsch-Gordan coefficients for different transitions. This induces light shifts and produces a periodic optical potential structure such that the shape of the light-induced potentials is the same for the two ground state sublevels, but the potentials are shifted spatially with respect to each other by $\lambda_L/4$, see Fig. 2. The top of the optical potential for one sublevel coincides with the bottom of the other one.

When the atomic motion occurs in a suitable velocity range, optical pumping of the atom between the ground state sublevels reduces the kinetic energy of the atom [2]. In this case quantum jumps and optical pumping to another ground state sublevel tend to occur when the atom is near the top of the optical potential. The atom is transferred to the bottom of another potential due to spontaneous emission and a consequent quantum jump.

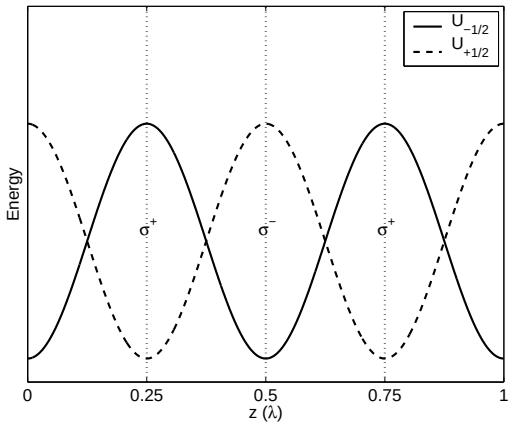

Figure 2: Schematic view of the optical potentials for the two ground state Zeeman sublevels in a red-detuned lattice with the atomic level structure $J_g = 1/2, J_e = 3/2$. The lattice structure is created due to the periodic polarization gradient of the laser field, and the points of pure circular polarization are indicated by dotted lines.

The subsequently emitted photon has a larger energy than the absorbed one, and the kinetic energy of the atom is therefore reduced, and the atom is cooled. After several such cooling cycles the atom localizes into the optical potential well, i.e., into an optical lattice site. Figure 3 shows the optical pumping cycles between the ground state sublevels cooling an atom, and the oscillations of the atomic wave packet after localization into an optical lattice site.

The intensity of the laser field and the strength of the coupling between the field and the atom is described by the Rabi frequency

$$\Omega = 2d\mathcal{E}_0/\hbar, \tag{5}$$

where d is the atomic dipole moment of the strongest transition between the ground and excited states. The detuning of the laser field from the atomic resonance is given by

$$\delta = \omega_L - \omega_0, \tag{6}$$

where ω_0 is the atomic resonance frequency. As a unit for Ω and δ the atomic linewidth Γ is commonly used.

The Hamiltonian for a single atom moving in the laser field given in

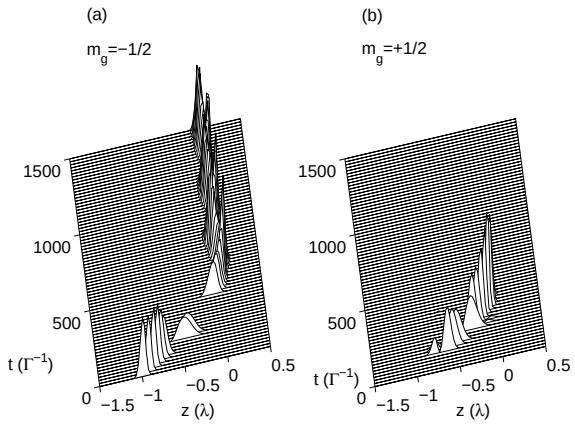

Figure 3: Sisyphus cooling and the localization of an atom into the optical lattice. A possible time evolution for a single atom wave packet is shown for two ground state Zeeman levels: (a) $m_g = -1/2$ and (b) $m_g = +1/2$. The result shows the optical pumping cycles and the localization of a single atom into the optical lattice. The discontinuous changes between the two ground states are due to quantum jump events from the excited state (not shown), selected to happen randomly with an appropriately weighted probability. If the run is repeated, the jumps would appear at different times.

Eq.(4) is after the rotating wave approximation

$$H = \frac{p^2}{2M} - \hbar\delta P_e + V. \tag{7}$$

Here, $p^2/2M$ is the kinetic energy, δ the detuning of the laser, $P_e = \sum_{m=-3/2}^{3/2} |e_m\rangle \langle e_m|$ is the projection operator onto the excited state, and the interaction between a single atom and the field is

$$\begin{aligned} V &= -i\frac{\hbar\Omega}{\sqrt{2}}\sin(kz)\left\{|e_{3/2}\rangle\langle g_{1/2}| + \frac{1}{\sqrt{3}}|e_{1/2}\rangle\langle g_{-1/2}|\right\} \\ &\quad + \frac{\hbar\Omega}{\sqrt{2}}\cos(kz)\left\{|e_{-3/2}\rangle\langle g_{-1/2}| + \frac{1}{\sqrt{3}}|e_{-1/2}\rangle\langle g_{1/2}|\right\} + H.c., \end{aligned} \tag{8}$$

where z is the position operator of the atom.

The modulation depth of the lattice is given by

$$U_0 = -\frac{2}{3}\hbar\delta s_0, \tag{9}$$

where s_0 is the saturation parameter

$$s_0 = \frac{\Omega^2/2}{\delta^2 + \Gamma^2/4}. \tag{10}$$

The spatially modulated optical potentials are

$$\begin{aligned} U_- &= U_0 \sin^2(k_r z), \\ U_+ &= U_0 \cos^2(k_r z), \end{aligned} \tag{11}$$

for ground states $m_g = -1/2$ and $m_g = +1/2$, respectively [38].

3.1.2 Localization in lattice

When the steady state is reached after a certain period of cooling, atoms are, to a large extent, localized into the lattice sites. In our studies of cold collisions with near-resonant optical lattices, the laser field is detuned a few atomic linewidths below (Papers I, II, and IV) or above (Paper III) the atomic transition. The optical lattice is in the oscillating regime if the atom completes on average more than one oscillation in the site before being optically pumped to a neighboring site. For less than one average oscillation per site, the lattice is in the jumping regime. The laser parameters Ω and δ determine in which of the regimes the lattice is in [38][8]. It must be noted that tight localization and occupation of the lowest vibrational levels of a periodic lattice potential increases the optical pumping time, and the time of localization within a single lattice site becomes longer compared to the semiclassical values [2]. Since we are mainly interested in the case when the two atoms undergo an intra-well collision, the chosen parameters in the work presented in this thesis correspond to the jumping regime of the lattice.

3.2 Blue-detuned optical lattices

In red-detuned lattices atoms are trapped around those spatial space points where the coupling between the ground and excited states has a maximum value, and consequently the number of scattered photons is large. It would be possible to reduce photon scattering if the atoms could be trapped around the points where the atom-laser coupling has a minimum value. This is indeed the case when the sign of the detuning is set to the blue side

[8]For an experimental study of the jumping regime of optical lattices with a slightly different laser field configuration, see Ref. [39].

of the atomic transition, $\delta > 0$, and, e.g., the atomic level configuration $J_e = J_g$ or $J_e = J_g - 1$ is used instead of the $J_e = J_g + 1$ configuration typical for the red-detuned case.

Hence the original motivation for the study of the blue-detuned polarization gradient cooling and trapping mechanisms was their ability to exploit the dark states to increase the phase space density, either directly by reducing the unwanted effects of reabsorption of scattered photons, or by feeding the once cooled atoms to sub-recoil cooling. The latter is possible since the blue-detuned polarization gradient and velocity selective coherent population trapping (VSCPT) subrecoil cooling schemes may coexist for the same atomic system, see Refs. [40, 41][9].

Two counterpropagating orthogonally polarized blue-detuned laser beams can efficiently cool down atoms which have the level structure $J_e = J_g$ or $J_e = J_g - 1$. The lowest position-dependent eigenstate of the system becomes now completely flat and is not coupled to the light field at any point of space. Thus despite of the cooling, the atoms are not trapped. The cooling works efficiently for atoms which have $J_g > 1$ since the flat dark state is not an eigenstate of the momentum operator, and there exists a motional coupling to the non-dark states. This coupling is largest when the non-flat state is energetically closest to the flat state. The consequence is the transfer of the population from the dark state to the spatially modulated state in the vicinity of the optical potential well, and subsequent Sisyphus-type cooling mechanism [4].

The obvious drawback in this case is the lack of a periodic trapping potential. The problem can be circumvented by the use of either transverse [45] or longitudinal [46] magnetic fields with respect to the laser propagation axis[10]. We have used in our studies the proposal of Grynberg and Courtois with a magnetic field along the laser axis [48], and I present this scheme in more detail in the following Section.

3.2.1 Grynberg-Courtois gray optical lattice

An applied longitudinal magnetic field removes the degeneracy of the atomic states of blue-detuned optical molasses described above, and produces the

[9] These schemes use a laser configuration where the counterpropagating laser beams have a non-orthogonal angle between their polarizations, instead of the typical orthogonal one used in the red-detuning case. For this scheme see also Refs. [42–44].

[10] There exists also a proposal and an experiment creating blue-detuned lattice by all-optical means, but this scheme uses two excited state hyperfine manifolds instead of only one [47].

necessary spatial modulation for the optical potentials and the lattice structure. This is easy to understand by considering the point in space where the laser field has a pure circular polarization. For σ^+ polarized light the ground Zeeman state $m_g = +J_g$ is not coupled to light when $J_e = J_g$ or $J_e = J_g - 1$, and the same applies for $m_g = -J_g$ in the point of σ^- polarization of the light field. The two states $m_g = \pm 1$ have opposite but equally large Zeeman shifts

$$\hbar\Omega_B = |\mu B|, \tag{12}$$

where μ is the magnetic moment of the corresponding state and the magnetic field strength is $B = B_z$ along the quantization axis z. The consequence is removal of the completely dark and flat lowest state with the spatially modulated lattice potential.

It is easy to vary the strength of the Zeeman shift $\hbar\Omega_B$ with respect to the light shift U_0 caused by the lasers. Obviously the two extreme regimes are: a) the Zeeman shift is small compared to the light shift $\hbar\Omega_B \ll U_0$, b) the light shift is small compared to the Zeeman shift $U_0 \ll \hbar\Omega_B$.

In case a), where the light shift dominates, the behavior of the lattice is paramagnetic. With the increasing magnetic field strength the lattice modulation becomes deeper. In this case the atoms are trapped only to the points of σ^- or σ^+ polarization of the laser field depending on the direction of the magnetic field. Due to the opposite Zeeman shifts only one of the two circular polarization points correspond to potential minima, and the period of the trapping potential is $\lambda/2$.

When the Zeeman shift dominates in the case b), the laser field produces perturbations to the Zeeman shifted states, and the situation resembles the traditional Sisyphus cooling scheme [2]. The optical pumping between the ground sublevels cools the atom which can be trapped in many internal states, causing an antiparamagnetic behaviour.

We have done our collision studies in this antiparamagnetic regime. See Fig. 4 for the used atomic level configuration $J_e = J_g = 1$ and Fig. 5 for the corresponding optical lattice structure. We label the three ground state sublevels with $|g_{\pm 1}>, |g_0>$, and the three excited state sublevels with $|e_{\pm 1}>, |e_0>$, where the integer subscripts indicate the angular momentum projection quantum number m along z-axis. Because the standing laser field has only circular components, and the Clebsch-Gordan coefficient between $m_e = 0$ and $m_g = 0$ states is zero, the atoms are rapidly pumped to the Λ subsystem of the whole state structure; thus, in this level configuration, the atoms are trapped to the ground substates which have an angular momentum quantum number $m_g = -1$ and $m_g = +1$. The excited state

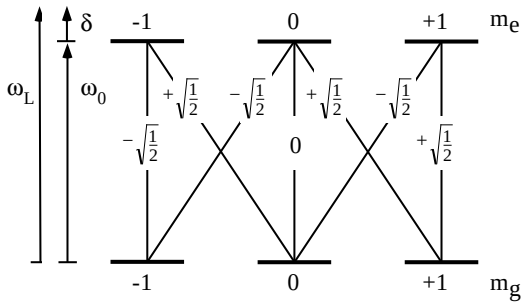

Figure 4: The level structure of a single atom for a blue-detuned lattice with the Clebsch-Gordan coefficients of corresponding transitions. This structure corresponds to particular hyperfine states of ^{87}Rb and can be used for efficient cooling and trapping of atoms in the Grynberg-Courtois blue-detuned lattice in the antiparamagnetic regime [48].

with $m_e = 0$ provides a way for cooling optical pumping cycles between the two trapping ground substates.

The modulation depth of the lattice is in this case given by

$$U_0 = \frac{1}{2}\hbar\delta s_0, \tag{13}$$

where the saturation parameter s_0 includes the Rabi frequency

$$\Omega = 2d\mathcal{E}_0/\sqrt{2}\hbar. \tag{14}$$

Here the Clebsch-Gordan coefficient which has an equal absolute value for all the allowed transitions is included in the definition of Ω.

After the rotating wave approximation the Hamiltonian for the atomic system interacting with the laser field given in Eq. (4) is

$$H = \frac{p^2}{2M} - \hbar\delta P_e + V + U. \tag{15}$$

Here, $P_e = \sum_{m=-1}^{1} |e_m\rangle \langle e_m|$ is the projection operator, and the interaction between a single atom and the field is

$$\begin{aligned} V &= i\frac{\hbar\Omega}{\sqrt{2}}\sin(kz)\{|e_0\rangle \langle g_{-1}| + |e_1\rangle\langle g_0|\} \\ &\quad + \frac{\hbar\Omega}{\sqrt{2}}\cos(kz)\{|e_{-1}\rangle\langle g_0| + |e_0\rangle\langle g_1|\} + H.c., \end{aligned} \tag{16}$$

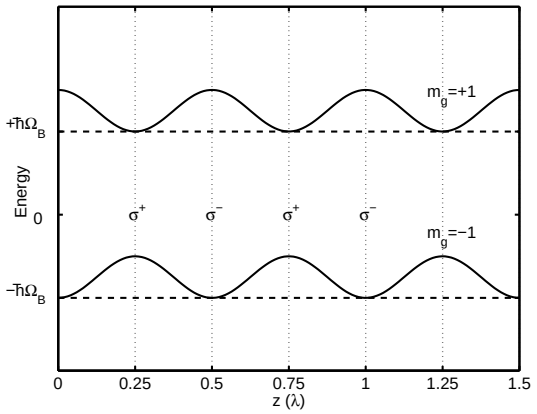

Figure 5: Schematic view of the optical potentials for the two trapping ground state Zeeman sublevels in a blue-detuned lattice. The periodic polarization gradient of the laser field creates the lattice structure and the points of circular polarizations are indicated by σ^+ and σ^-. The dashed lines give the Zeeman shifted energy levels which the light field modifies.

where z is the position operator of the atom. The interaction with a magnetic field in Eq. (15) is

$$U = \sum_i m_i \hbar \Omega_{B_i} |i\rangle\langle i|, \tag{17}$$

where the sum over i includes all the ground and excited states, and the Zeeman shift factors Ω_{B_i} are for the two tapping ground substates $m = \pm 1$ equal to Ω_B.

The level structure which we have used in our studies for a blue-detuned lattice can be found in ^{87}Rb, which has $F = 1$ hyperfine states for both the $5S_{1/2}$ ground state and the $5P_{1/2}$ excited state[11].

The reason for the choice we have made for the used level structure and an antiparamagnetic regime of the Grynberg-Courtois lattice is in their simplicity. The cooling mechanism resembles the traditional Sisyphus cooling, making it more relevant to compare the results between the red and blue-detuning studies. Moreover, it is necessary to use only three levels of the Λ-subsystem instead of all the six levels of a single atom. Thus the number of product state basis vectors for interaction studies between the

[11]This is actually the element and the level scheme which has been used in the blue-detuned lattice experiment of Hemmerich *et al.* [45], even though in their case the lattice structure and the orientation of the magnetic field differs from what is presented here.

atoms can be reduced in the blue-detuned case. This reduces the computational resource requirements and speeds up the simulations when compared to red-detuned case (which has to use all the six substates of a single atom for the interaction studies). Thus for blue-detuned lattices it is easier to make a wider exploration of parameter space, if required.

3.3 Basic theoretical approach

The essence of Sisyphus cooling is optical pumping between the various internal states of an atom and it can not be treated as a simple two state system consisting of only a single ground and a single excited state. Because of the polarization gradients, the laser couples the multitude of Zeeman substates of the atom in a position-dependent way and the spontaneous emission caused by the coupling to the vacuum plays a crucial role in the optical pumping process.

Thus to describe the atomic motion in optical lattices one has to solve the problem of a multi-level atom coupled to a monochromatic laser field and to a quantized electromagnetic environment in its vacuum state.

It is possible to treat the external laser field classically since the fields which are considered weak from the Sisyphus cooling and the lattice point of view still contain a large number of photons[12]. Moreover, the treatment of the interaction between a classical field and an atom is typically done by using the rotating wave approximation, which neglects the terms that do not conserve the total energy.

The general form of the task is to solve the density matrix master equation

$$i\hbar\frac{d\rho}{dt} = [H, \rho] + \mathcal{L}_{rel}[\rho], \tag{18}$$

where H is the atomic system Hamiltonian, see Eqs. (7) and (15), and $\mathcal{L}$ includes the spontaneous emission part due to the coupling to the environment.

It is not possible to solve this equation analytically even in the case of the simplest atomic level schemes used for optical lattices. One can try to find approximations which allow an analytical treatment, or the combination of analytical and numerical calculations to Eq. (18). Another possibility is to simulate the optical lattice system on a computer, especially,

[12]Typical laser intensities used in experiments are a few mW/cm^2. Of course, when laser cooled atoms are injected into cavities, the coupling field is quantized, e.g., see an experiment where atomic trajectories are modified by single photons [49], or a proposal to manipulate cold collisions by cavity QED effects [50].

simulations by the Monte Carlo wave-function (MCWF) method may provide a convenient way to obtain the solution of Eq. (18) [51–54].

A common feature for analytical treatments of optical lattices is the adiabatic elimination of the excited states, thus reducing the number of the levels in the problem at hand [6]. One can then try to solve the master equation directly by numerical integration, introduce further approximations, or exploit the translational symmetry properties of the system [55]. Short introductions to the various approaches can be found in review articles [3] and [6].

The MCWF method was originally developed for problems in quantum optics, where in many of the cases the direct quantum-mechanical solution of the system density matrix is very difficult or impossible to obtain[13]. For example, in the case of laser cooling, one can develop combinations of analytical and numerical treatments to treat 2D case [60], but the 3D problem has been solved so far only by MCWF simulations [57]. The difficulty usually arises because of a large number of system density matrix elements, or a large number of degrees of freedom of the environment to which the system is coupled. The key idea of the method is the generation of a large number of single wave function histories which include stochastic quantum jumps of the system studied. The final result for the system density matrix and the system properties can then be calculated as ensemble averages of single histories.

We have chosen for our collision studies in optical lattices the MCWF method since it has been a widely used benchmark method for various semiclassical theories in the field of cold collisions in MOTs [61]. The method gives a full quantum-mechanical description of the atomic system[14], and treats spontaneous decay in a rigorous way. A semiclassical version of the Monte Carlo (MC) method has also been developed for lattice studies [62]. This variant describes the external atomic degrees of freedom classically, and is not valid when the spread of the wave packet influences the dynamics of the system. This is the case when an atom is tightly localized into a lattice site and the spread of the packet affects essentially the optical pumping rate. Moreover, the semiclassical approach can not treat, e.g., the

[13]Problems which are solved with the aid of the MCWF method in quantum optics can vary e.g. from the resonance fluorescence spectrum of 1D optical molasses [56] to 3D laser cooling [57] and heating of a trapped ion [58]. For more examples, see Ref. [54]. By now the method has also been applied outside the field of quantum optics, into transport problems in condensed matter physics [59].

[14]The external laser field is still described classically.

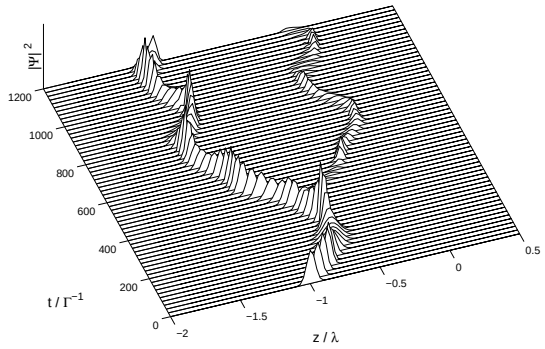

Figure 6: Branching of a wave packet. The time evolution of the total atomic wave packet in position space is shown. In addition to treating spontaneous decay in a rigorous way, the full quantum-mechanical MCWF method can also account for the branching of the wave packet shown here (unpublished).

branching of the wave packet in optical lattice shown in Fig. 6[15].

Previously developed analytical quantum-mechanical models for non-interacting atoms in optical lattices become impossible to solve if we want to find out the consequences of the dynamical interaction processes, that is cold collisions, to the system dynamics. It is fairly simple to do MCWF studies for a single atom moving in one-dimensional optical lattice, see Figs. 3 and 6. Simulations become computationally heavy and are not straightforward when describing interactions between moving atoms in optical lattices. I give a detailed description of the formulation by MCWF method of our lattice problem for interacting atoms in Chapter 5. Paper IV presents some ideas how it might be possible to simplify the full quantum-mechanical benchmarking methods by combining semi-classical and quantum methods for lattice studies.

3.4 Variety of optical lattice designs

In our studies we have used for simplicity the 1D lin⊥lin laser configuration. In this case the standing wave has only circular polarization components, and the change of the relative phase between the two counterpropagating and orthogonally polarized laser beams simply translates the lattice spatially.

[15]For the branching of the packets, see e.g. discussion in Ref. [63].

For lattices in two and three dimensions there are basically two different approaches which are in the literature sometimes referred as Grynberg [15, 64] or Hänsch [16, 65] style lattices. The essential difference between the two is in the consequence of the number of laser beams.

In Grynberg style $n = d+1$ beams are used. Here d is the dimensionality of the spatial space, and n the number of the used beams. In this case, there are d independent relative phases of the beams. If the phases fluctuate in time, the consequence is simply a translation of the lattice in space. In experiments the fluctuations in the phases of the beams are much slower than the time scale for the dynamics of the atoms trapped in a lattice. Thus the atoms follow adiabatically the translation of the lattice, and the phases of the laser beams need not to be locked.

If the number of the used beams is more than $d + 1$, there are more independent relative phases between the lasers than there are spatial dimensions. An obvious and unavoidable consequence is the change in the topology of the lattice with fluctuating phases of the lasers. Hence, if more than $d+1$ beams are used, the phases of the lasers need to be locked. This is the case for Hänsch style lattice.

The crystal structure in lattices can vary, e.g., from a body and a face centered cubic lattices [64] to quasiperiodic lattices [66]. It is a great benefit to easily create a variety of structures by controlling the lattice parameters in a simple way.

3.5 About applications of optical lattices

It is not possible to describe here in detail the development of the ideas and the experiments dealing with optical lattices. These may vary e.g. from the observation of Bragg scattering of light from a sparsely filled optical lattice [30,31] and observation of Bloch oscillations [32] to the use of lattice bound atoms as a quantum simulator [67] or to dynamical tunneling [35]. From the technological application point of view the experimental realization of a deterministic source and delivery of a single atom using an optical lattice may be of interest [68]. Detailed descriptions of the development of the ideas and the experiments can be found in the review articles [3–6].

Recently it has become possible to achieve high atomic occupation densities in far off-resonant optical lattices [69, 70][16]. The loading of the lattice with a BEC [71–73] has allowed many delicate experiments involving

[16] In far off-resonant lattices the photon scattering is negligible and the atom-laser coupling provides a conservative trapping potential for the atoms.

quantum coherences [29, 35, 74–76][17]. Especially the recent observation of the quantum phase transition between a superfluid and a Mott-insulator opens many new possibilities [79], e.g., filling the lattice with a controlled number of particles per lattice site. This can make the proposals of performing quantum computation in optical lattices more realistic [80, 81], or it may allow the making of a molecular BEC [82, 83] by melting the Mott-insulator [84].

Some other recent ideas and experiments related to optical lattices include having an atomic BEC directly in optical lattice without the preliminary magnetic cooling steps [85], inducing a BCS transition in a fermion-loaded lattice [86], particle number fractionalization [87], and feedback control of atoms in optical lattices [88].

[17] See also the comment [77] on Ref. [74] and reply [78].

4 Cold collisions between laser cooled atoms

The thermal velocities of laser cooled gaseous atoms are roughly centimeters per second. Because of the slow motion, the collision dynamics is strikingly different when compared to room temperature atoms. In other words, the kinetic energies involved in the cold collision process are on the order or less than the energy of the atomic linewidth. For example, in the case of cesium the linewidth of a typical cooling transition is $2400\mathrm{E}_r$ and a typical collision energy is around $1600\mathrm{E}_r$. This also means that the decay time of the excitation becomes small compared to the time scale of the total collision dynamics. This allows new phenomena in cold collision processes to affect the thermodynamics of the cold atomic cloud [7,8]. A great benefit of slow atomic motion is that it allows very precise spectroscopical studies of atomic properties with cold atom gases [8].

A general categorization can be made by considering collisions occuring between two ground state or between one ground and one excited state atom. Here I describe binary collisions between atoms of same element, i.e., a homonuclear diatomic molecule, and the emphasis is on the collisions between a ground and an excited state atom. This is relevant for the case with the presence of near-resonant light, which is the case in our lattice studies.

The collisions between ground state atoms occur in a very short range of atomic distances and the collision properties are important in defining the efficiency of the magnetic evaporative cooling, a necessary step when forming a BEC in a magnetic trap. In such case, inelastic collisions which change the hyperfine state of the colliding atoms lead to a loss of atoms from the trap.

In the presence of near-resonant light the excitation of a quasimolecule formed by the colliding atoms may occur at extremely long range, even on the order of few thousands of Bohr radii a_0. Molecular potentials at these long ranges are usually labeled by the Hund's case (c) notation, where the component of the total electronic angular momentum along the internuclear axis is a good quantum number[18]. The electron clouds of the colliding atoms do not overlap at longe range, and the dominant interaction between the atoms is the resonant dipole-dipole interaction. I give a more detailed description of the resonant dipole-dipole interaction in Section 5.1, and previous calculations for alkali-metals can be found in Refs. [90, 91].

[18] For a clear presentation of various Hund's coupling cases see e.g. Ref. [89]. See also Fig. 11 for an example of attractive potentials at long range.

The long range properties of molecular states and the sign of the detuning of the laser define the possible consequences of collisions. A repulsive or an attractive character of the molecular potential at long range arises due to the relative orientation of the dipole moments of the colliding atoms. In the case of a red-detuned laser, the resonance or Condon point r_c, occurs for an attractive state. For a blue-detuned laser r_c occurs for a repulsive state. Depending on the magnitude of the detuning and the strength of the coupling laser, off-resonant excitation to non-resonant state may also play a role, see Paper III.

A lively research field of its own is the photoassociation of laser cooled atoms to molecules. This is typically done by using a large red detuning of the laser so that free atom pair is excited at r_c to a well defined bound molecular vibrational state. Photoassociation has provided important contributions when precise data on atomic interaction potentials or the values of s-wave scattering lenghts for BEC studies have been obtained [8]. A great deal of study has also been done on the photoassociation in an atomic Bose-Einstein condensate [82, 83, 92]. I will not discuss further the field of photoassociation but the reader can find presentations of the field from Refs. [8, 93].

4.1 Radiative heating by red-detuned light

With red-detuned light, the population of the quasimolecule formed by the two collision partners may get resonantly excited into an attractive excited state at the Condon point r_c (see Fig. 7). The relative velocity of the atoms increases due to the acceleration on the attractive state until spontaneous emission terminates the process. When the atoms have again bounced apart due to the short range repulsion in the ground state, the pair may lose some of the gained kinetic energy in the reverse process. Anyhow, the overall effect is the heating of the colliding pair, and the escape of the atoms from the trap if the total gain in kinetic energy is large enough [8].

Figure 7 shows a semiclassical (SC) schematic view of the process. In some of the parameter regimes SC descriptions, such as the Landau-Zener level crossing model, can be used [61]. When the SC models fail, full quantum-mechanical methods are needed. For example, MCWF simulations [94, 95] can be used as a benchmark method for easier analytical semiclassical calculations. It should be emphasized that it is difficult in SC models to account for population recycling, which means that once-decayed population may get re-excited in strong laser fields. A comparison between various methods and their application range is given in Ref. [61].

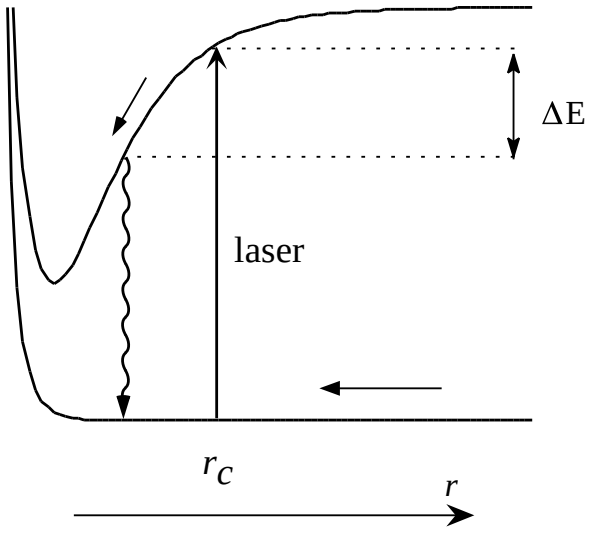

Figure 7: A schematic view of radiative heating of colliding atoms. The quasimolecule is excited at the Condon point r_c and accelerated on the upper level before spontaneous decay terminates the process.

Most of the radiative heating studies done so far have used a simple two-state description with one ground and one excited molecular electronic state. An example of MCWF simulation results for MOT from Ref. [95] is shown in Fig. 8. The results show clearly the effect of radiative heating and consequent spreading of the momentum distributions. I emphasize that our lattice studies include many attractive and repulsive states simultaneously, see Section 5.1.

In addition to radiative heating, atoms may also escape from the trap by the fine-structure change mechanism. If the population survives on the excited state for small enough relative distance between the two atoms, the point where two fine-structure states have a crossing may be reached. Now, if the pair comes out from a collision region in an energetically lower fine-structure state than the one in which they entered the collision, the pair gains kinetic energy by the amount corresponding to the fine-structure splitting of the states at large r. This energy difference is usually large compared to the trap depths, and consequently in this case the atoms escape from the trap [7, 8].

We deal in our studies with very small detunings, a few atomic linewidths

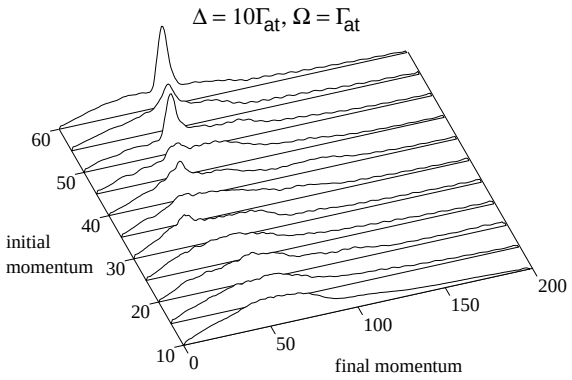

Figure 8: An example of radiative heating study in MOT from Ref. [95]. Final momentum distributions for various initial values of a narrow Gaussian momentum distributions are shown. The effects of radiative heating, the spreading of the distributions, and the momentum increase is clearly visible, especially for low initial relative momentum. For higher initial momentum some character of the initial distribution is still preserved in the post-collision distribution.

only[19], and strong laser fields. It is therefore reasonable to assume that the effect of fine-structure changing collisions is very small compared to effect of radiative heating processes, and we neglect the fine-structure change loss mechanism in our lattice studies.

4.2 Optical shielding by blue-detuned light

When blue-detuned light is used, the resonant excitation at the Condon point occurs to a repulsive excited quasimolecular state. This makes it possible to shield the atoms from close encounters [8], see Fig. 9. If the shielding is efficient, collisions between atoms may become completely elastic. The mechanism would obviously be useful for preventing loss of atoms in optical lattices formed with a blue-detuned light.

In an optical shielding process, resonantly excited quasimolecule population reaches the classical turning point on the repulsive excited state and the atoms begin to move apart again. The shielding becomes complete if all the population has been excited, no spontaneous decay has occurred, and all the population returns resonantly to the ground state at the Condon

[19]There can be an order of magnitude difference between the fine-structure state crossing point and r_c for the small detunings we have used.

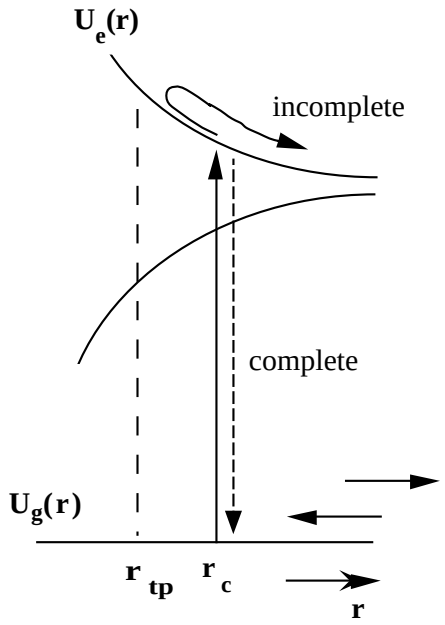

Figure 9: A schematic semiclassical presentation of optical shielding. The quasimolecule is excited resonantly to the repulsive molecular state at the Condon point r_c. Then it reaches the classical turning point r_{tp}, and is finally transferred back to the ground state when arriving at r_c again. If the transfer back to the ground state is not complete, the atom pair may gain kinetic energy as it is further accelerated by the excited state potential. In this case shielding is incomplete and the collision is inelastic. If the population transfer between the states is adiabatic, shielding is complete and the collision between the atoms is elastic.

point. In this case, collisions become elastic (when photon recoil effects are ignored), and no heating or escape occurs due to inelastic processes. Moreover, the ground state is emptied at a relatively long range, and no population reaches short distances where unwanted processes are possible, such as hyperfine state changing collisions. Thus, the possibility to use optical shielding in an efficient way allows further increase in the occupation density of the lattice, in addition to the benefits of the reduced rate of scattered and reabsorbed photons that are characteristic for the blue-detuned lattices.

In the past MCWF simulations have described the efficiency of the

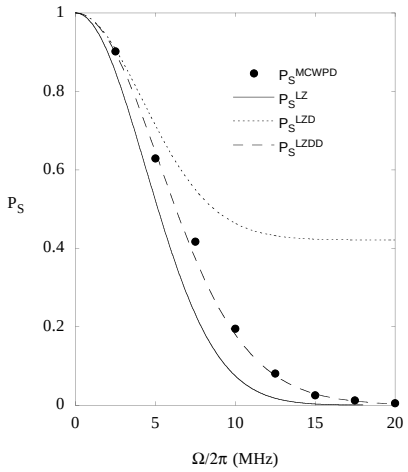

Figure 10: An example of an optical shielding study in a MOT from Ref. [25]. Shown is the shielding measure P_S as the function of the Rabi frequency Ω. P_S describes the ground state population flux at very short range. The dots are results of the Monte Carlo simulations and the lines presents the results of various semiclassical Landau-Zener approaches. When the laser field is strong enough, the ground state is effectively emptied before the atoms have a chance to approach close to each other.

shielding process by a shielding measure P_S, which essentially describes the flux of the ground state population to the short range beyond the Condon point r_c [25, 96, 97], see Fig. 10. In the case of optical lattices, a more descriptive result is the momentum distribution in a steady state compared between interacting and non-interacting atoms, see Paper III. We have also combined the cooling and shielding dynamics in a single framework, which has not been done before to our knowledge.

In this Chapter we have described radiative heating and optical shielding processes by using the molecular state description. This is how the treatment has usually been done in the past when studying the heating and loss of atoms in MOTs. In our calculations and simulations we use the two-atom product state presentation instead. Our aim is to study the effect of collisions in a near-resonant optical lattice. Most of the photon scattering still occurs when the atoms are outside the range of a binary interaction. It would be an unnecessary complication to describe photon scattering and quantum jumps in a lattice by using a molecular basis. Moreover, we give a simultaneous description for laser cooling and collision processes. Hence,

in our case the molecular basis is only used for a qualitative description of radiative heating and optical shielding processes, but it does not appear directly in our calculations.

A wide overview of the theoretical approaches for radiative heating and optical shielding is given in Ref. [8].

5 Collisions in optical lattices

In the past cold binary collisions between atoms have been widely studied under conditions which correspond to the atoms trapped in magneto-optical traps [7, 8, 17]. Previous cold collision research has concentrated on the effects of inelastic collisions on the properties of an atomic cloud, but has neglected the co-existence of the cooling processes.

We are dealing with near-resonant optical lattices, and we have combined in a single framework the Sisyphus cooling mechanism and cold collision dynamics[20]. Thus our approach includes simultaneous dynamical processes of cooling, trapping, and collisions in a gaseous atomic cloud.

Radiative heating and optical shielding studies in MOTs typically use the molecular state description of the binary atomic system. After choosing the specific excited molecular state and doing the partial wave expansion, usually only the lowest relative angular momentum ground and excited state are accounted[21]. Thus the descriptions in the past have been two-state models, neglecting the multitude of internal states of the atoms, and without the position dependent coupling between the atoms and the laser field. For optical lattices the internal states of the atoms have to be accounted because of the spatial periodicity of the coupling caused by the polarization gradients of the laser field. The system under study thus becomes very complex and the requirement for computation time of the simulations increases greatly, see Appendix B.

We use the two-atom product state basis [98]. For two six-level atoms in the red-detuned case this means 36 basis states. If the basis is transformed into a molecular one, there are manifolds of attractive and repulsive molecular states buried in our description. We are forced to do the calculations in one dimension since the finite amount of computational resources.

A resonant dipole-dipole interaction between the atoms in optical lattices has been studied by some groups recently with nondynamic approaches [99–103]. Usually these studies assume fixed positions for the atoms and concentrate on the mean-field type descriptions of the lattice system. These approaches neglect the dynamical nature of the cold collisions, and the in-

[20] For far off-resonant lattices the possibility to control the cold collisions coherently has been proposed [81]. This would allow the creation of an entanglement between the atoms, and the use of atoms trapped in optical lattices for quantum computing. A step making the proposal more realistic was done recently by the experiment presented in Ref. [79].

[21] Or independent pairs of partial wave states, neglecting the coupling between the pairs in a weak field approximation [95].

elastic processes of radiative heating or incomplete optical shielding. To our knowledge, our studies are the only ones that include the dynamical processes of Sisyphus cooling and cold collisions in the same framework. It is important to note that once the atoms are localized into the optical lattice sites, they are still able to move around in the lattice. For shallow lattices this is because the quantum-mechanical tunneling probability between the lattice sites is not negligible. For deep optical lattices, which are more relevant to our case, the atomic motion between the wells may be induced by the recoil effects combined with the optical pumping process. An atomic wave packet has a finite width, and thus a finite probability in the center of the lattice site to be excited to the state from where spontaneous decay may take it to another ground substate. The corresponding optical potential in this case has a potential peak instead of a potential well around that particular point in space.

For the lattice parameters we use, we have noticed that inter-well effects are negligible and our interest lies in the case when two atoms end up in the same lattice site and collide. The intra-well collision partners may then gain kinetic energy due to an inelastic collision and escape from the lattice. In the case of optical shielding, the possibility of making the collisions elastic and preventing the atoms from close encounters would not allow the atoms to escape from the lattice.

Numerical simulations are extremely heavy, especially in the case of red-detuned lattices where the level scheme can not be simplified. Thus we are forced to make some simplifications to our model. The details of these are recorded in Paper II. Most importantly, we have to neglect the reabsorption of the scattered photons. With increasing atomic density, reabsorption may heat-up the atomic cloud and cause radiation pressure to outward direction from the trap center [9], limiting the achievable atomic densities. In the blue-detuned lattice, the number of scattered photons is largely reduced because the center of each lattice site corresponds to a completely dark point in space. For red-detuned lattices we merely describe the effects of collisions on the thermodynamical properties of the cloud. The full thermodynamics is not described since we neglect reabsorption. This poses some limitations for the applicability of our results in red-detuned lattices, but for the blue-detuned case our description is close to the complete thermodynamical description because the scattering is generally low.

We have to also fix the position of one of the colliding atoms which reduces the dimensionality of the problem from an impossible two to tractable one. The inelastic interaction process will not change the kinetic energy of

both atoms, but we use the relative kinetic energy as an estimate for the kinetic energy change per atom.

In the following Section I describe how we calculate the interaction matrix elements between two multistate atoms, especially the resonant dipole-dipole interaction matrix elements. The whole problem is then formulated by using the MCWF method. At the first look, one might think that the application of the MCWF method would be straightforward for the problem at hand. This is not the case. I will not present all the details here, but refer to Paper II. This Chapter ends with the presentation of the central results.

5.1 Resonant dipole-dipole interaction

One of the early treatments for resonant dipole-dipole forces between two atoms was given already at the end of the 30's [104], and the retardation effects were discussed almost a decade later [105].

The resonant dipole-dipole interaction (DDI) is the first interaction to come into play when the colliding atoms approach each other. It arises via the coupling of the atoms to the quantized environment. Our derivation follows the approach of Lenz and Meystre who considered two-level atoms in a standing-wave field [106].

Since the interaction between the atoms is mediated by the quantized environment, the natural starting point is the two-atom system master equation and its damping part describing the coupling of the system to the electromagnetic environment [106] [see also Eq. (18)]

$$\begin{aligned}\dot{\rho}|_{sf} &= -\frac{1}{\hbar^2}\int_0^t d\tau Tr_f \{H_{sf}(t)H_{sf}(\tau)\rho_{sf}(\tau) - H_{sf}(t)\rho_{sf}(\tau)H_{sf}(\tau) \\ &\quad -H_{sf}(\tau)\rho_{sf}(\tau)H_{sf}(t) + \rho_{sf}(\tau)H_{sf}(\tau)H_{sf}(t)\}\,, \qquad (19)\end{aligned}$$

where H_{sf} denotes the system-field interaction Hamiltonian, and Tr_f the trace over the field.

We expand the electromagnetic field in the standard way

$$\begin{aligned}\mathbf{E}(\mathbf{r}_\alpha) &= \mathbf{E}^+(\mathbf{r}_\alpha) + \mathbf{E}^-(\mathbf{r}_\alpha) \\ \mathbf{E}^+(\mathbf{r}_\alpha) &= \sum_{\mathbf{k}} i\mathcal{E}(\mathbf{k})\mathbf{a}_{\mathbf{k}} e^{i\mathbf{k}\cdot\mathbf{r}_\alpha} \\ \mathbf{E}^-(\mathbf{r}_\alpha) &= \left(\mathbf{E}^+(\mathbf{r}_\alpha)\right)^\dagger, \qquad (20)\end{aligned}$$

where $\mathbf{a}_{\mathbf{k}}$ is the annihilation operator for mode $\mathbf{k}$, $\mathbf{r}_\alpha$ denotes the position

of atom α, and

$$\mathcal{E}(\mathbf{k}) = \sqrt{\frac{2\pi\hbar\omega(\mathbf{k})}{V}}\epsilon_j(\mathbf{k}), \tag{21}$$

where ϵ_j is the polarization vector and V the quantization volume.

We use the center of mass and relative coordinates of the atom pair

$$\mathbf{R} = \frac{\mathbf{r}_1 + \mathbf{r}_2}{2}, \quad \mathbf{r} = \mathbf{r}_2 - \mathbf{r}_1, \tag{22}$$

and the notation

$$\begin{aligned} S_{+,q} &= \sum_m CG^q_m \left(|e_{m+q}\rangle_1\ {}_1\langle g_m| + |e_{m+q}\rangle_2\ {}_2\langle g_m|\right) \\ \Delta S_{+,q} &= \sum_m CG^q_m \left(|e_{m+q}\rangle_1\ {}_1\langle g_m| - |e_{m+q}\rangle_2\ {}_2\langle g_m|\right), \end{aligned} \tag{23}$$

where CG^q_m are the appropriate Clebsch-Gordan coefficients, q is the polarization label in the spherical basis, and sub-indices label the two atoms. The interaction between the two-atom system and the vacuum electromagnetic field can now be written as

$$\begin{aligned} H_{sf} = i\sum_{\mathbf{k},\epsilon_j}\sqrt{\frac{2\pi\hbar\omega(\mathbf{k})}{V}}d\Big\{&\epsilon_{j,+}\left[\cos\left(\mathbf{k}\cdot\frac{\mathbf{r}}{2}\right)S_{+,+} - i\sin\left(\mathbf{k}\cdot\frac{\mathbf{r}}{2}\right)\Delta S_{+,+}\right] \\ &+\epsilon_{j,0}\left[\cos\left(\mathbf{k}\cdot\frac{\mathbf{r}}{2}\right)S_{+,0} - i\sin\left(\mathbf{k}\cdot\frac{\mathbf{r}}{2}\right)\Delta S_{+,0}\right] \\ &+\epsilon_{j,-}\left[\cos\left(\mathbf{k}\cdot\frac{\mathbf{r}}{2}\right)S_{+,-} - i\sin\left(\mathbf{k}\cdot\frac{\mathbf{r}}{2}\right)\Delta S_{+,-}\right]\Big\}e^{i\mathbf{k}\cdot\mathbf{R}}e^{i\omega_0 t}\mathbf{a}_{\mathbf{k},j} \\ &+H.c., \end{aligned} \tag{24}$$

where $e_{j,q}$ is the projection $\epsilon_{j,q} = \epsilon_j \cdot \epsilon_q$ on the spherical basis $\epsilon_{\mathbf{0}}, \epsilon_{\pm}$, and d the dipole moment of the atomic transition.

One can identify the DDI interaction terms between the atoms as those having $< n_\omega + 1 >= 1$ where n_ω is the number of photons in the mode of the environment with mode frequency ω. In another words, the average photon number in the interaction process is zero since the DDI interaction can be viewed as an exchange of excitation between the two atoms via the environment vacuum field. After lengthy analytical calculations following [106], and using the arguments from Ref. [107], one can write down the expression for the three-dimensional resonant dipole-dipole interaction as

$$
\begin{aligned}
V_{dip} &= -\frac{3}{8}\hbar\Gamma\left\{\frac{1}{3}\frac{\cos q_0 r}{q_0 r}\left[1-2P_2(\cos\theta_r)\right]\left(\mathcal{S}_{++}\mathcal{S}_{-+}+\mathcal{S}_{+-}\mathcal{S}_{--}-2\mathcal{S}_{+0}\mathcal{S}_{-0}\right)\right. \\
&\quad -2\left[\frac{\sin q_0 r}{(q_0 r)^2}+\frac{\cos q_0 r}{(q_0 r)^3}\right]P_2(\cos\theta_r)\left(\mathcal{S}_{++}\mathcal{S}_{-+}+\mathcal{S}_{+-}\mathcal{S}_{--}-2\mathcal{S}_{+0}\mathcal{S}_{-0}\right) \\
&\quad +\frac{1}{3}\left[-\frac{\cos q_0 r}{q_0 r}+3\left(\frac{\sin q_0 r}{(q_0 r)^2}+\frac{\cos q_0 r}{(q_0 r)^3}\right)\right]\times \\
&\quad \left[\frac{1}{\sqrt{2}}P_2^1(\cos\theta_r)\cos\phi_r\left(-\mathcal{S}_{++}\mathcal{S}_{-0}+\mathcal{S}_{+0}\mathcal{S}_{--}-\mathcal{S}_{+0}\mathcal{S}_{-+}+\mathcal{S}_{+-}\mathcal{S}_{-0}\right)\right. \\
&\quad \left.\left.+P_2^2(\cos\theta_r)\cos 2\phi_r\ \left(\mathcal{S}_{++}\mathcal{S}_{--}+\mathcal{S}_{+-}\mathcal{S}_{-+}\right)\right]\right\}, \qquad (25)
\end{aligned}
$$

where $q_0 = \omega_0/c$, P_2 is Legendre polynomial, and P_m^n are the associated Legendre functions. The angles θ_r and ϕ_r are the angles of the relative coordinate $\mathbf{r}$ in the spherical basis. We have also introduced the operators

$$
\mathcal{S}_{+q}\mathcal{S}_{-q'} \equiv \left(S^1_{+,q}S^2_{-,q'}+S^2_{+,q}S^1_{-,q'}\right), \qquad (26)
$$

where $S^\alpha_{-,q} = \left(S^\alpha_{+,q}\right)^\dagger$ and

$$
S^\alpha_{+,q} = \sum_{m=-J_g}^{m=J_g} CG^q_m |e_{m+q}\rangle_\alpha\ {}_\alpha\langle g_m|. \qquad (27)
$$

Here α labels one of the two atoms.

If the two atoms are positioned on the z-axis, the DDI potential reduces to the one-dimensional potential

$$
\begin{aligned}
V_{dip}^{axis} &= \frac{3}{8}\hbar\Gamma\left\{\frac{1}{3}\frac{\cos q_0 r}{q_0 r}+2\left[\frac{\sin q_0 r}{(q_0 r)^2}+\frac{\cos q_0 r}{(q_0 r)^3}\right]\right\}\times \\
&\quad \left(\mathcal{S}_{++}\mathcal{S}_{-+}+\mathcal{S}_{+-}\mathcal{S}_{--}-2\mathcal{S}_{+0}\mathcal{S}_{-0}\right). \qquad (28)
\end{aligned}
$$

This is the expression which we have used in our calculations formulated in the two-atom product state basis. It is worth noting that the interaction potential (28) includes the retardation effects. By diagonalizing V_{dip}, it is possible to obtain the molecular potentials shown in Fig. 11. I emphasize again that the calculations are done in the two-atom product state basis for reasons described above, and the molecular basis is occasionally used only for the qualitative description of the collision processes.

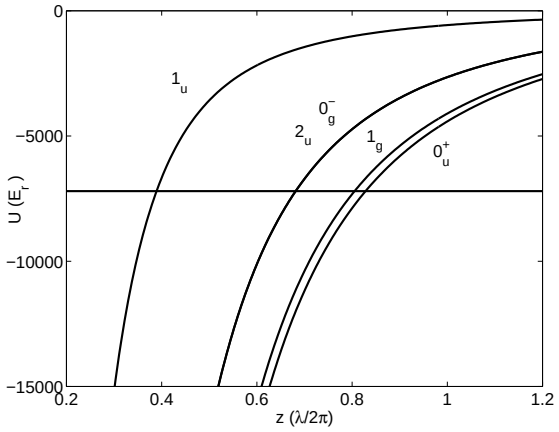

Figure 11: The energy shifted ground state and the attractive excited state [labeled by the Hund's case (c) notation] molecular potentials of Cs_2 for $\delta = -3.0\Gamma$. The repulsive potential manifold is not shown.

5.2 Monte Carlo wave-function formulation

We use a variant of the Monte Carlo (MC) method which was developed by Dalibard, Castin, and Mølmer [51–53]. The core idea of the Monte Carlo wave-function (MCWF) method is the generation of a large number of single wave function histories including stochastic quantum jumps of the system studied. Quantum jumps occur to the available decay channels of the system whose environment is constantly monitored. In our case, detection of a photon would correspond to a quantum jump from an internal excited state to the ground state of an atom in an optical lattice. Solutions for the steady state density matrix and system properties can then be calculated as ensemble averages of single wave-function histories.

In the simulations quantum jumps to the appropriate decay channels occur due to a non-Hermitian part in the total Hamiltonian. Thus, in order to generate the ensemble members, one solves the time dependent Schrödinger equation

$$i\hbar\frac{\partial|\psi\rangle}{\partial t} = H|\psi\rangle. \tag{29}$$

For the numerical propagation methods, see Appendix A.

We have to fix the position of one atom, as discussed in the beginning of this Chapter and Paper II. If the position of atom 1 is fixed, the binary system wave function in the two-atom product state basis depends now

only on the position of the moving atom 2

$$|\psi(z_2,t)\rangle = \sum_{j_1,j_2,m_1,m_2} \psi_{j_2,m_2}^{j_1,m_1}(z_2,t)|j_1 m_1\rangle_1 |j_2 m_2\rangle_2. \tag{30}$$

Here, j_1 and j_2 denote the ground and excited states of atom 1 and 2 respectively, m_1 and m_2 the z-component of the angular mometum, and z_2 the position of the moving atom 2 in the lattice. The atomic spatial dimensionality of the problem is reduced from two to one. The relative coordinate z between the atoms is now $z = z_2 - z_f$, where z_f is the position of the fixed atom.

The non-Hermitian Hamiltonian H in Eq. (29) for the two-atom system is

$$H = H_S + H_{DEC}, \tag{31}$$

where the system Hamiltonian H_S in our case includes the atom-laser interaction Hamiltonians expanded in the two-atom Hilbert space, and the resonant dipole-dipole interaction between the atoms, Eqs. (7,15,28).

The non-Hermitian part includes the sum over various decay channels j,

$$H_{DEC} = -\frac{i\hbar}{2} \sum_j C_j^\dagger C_j, \tag{32}$$

where C_j are the jump operators corresponding to particular decay channels.

During a discrete time evolution step of length δt the norm of the wave function may shrink due to H_{DEC}. The amount of shrinking gives the probability of a quantum jump to occur during the short interval δt. Based on a random number one then decides whether a quantum jump occurred or not. Before the next time step is taken, the wave function of the system is renormalized. If and when a jump occurs, one performs a rearrangement of the wave function components according to the jump operator C_j, corresponding to decay channel j, before renormalization of $|\psi\rangle$.

For example, if we denote the jump of atom 1 from $|e_{-1/2}\rangle_1$ to $|g_{-1/2}\rangle_1$ as channel 2 in our red-detuned lattice studies, the jump operator in the product state basis for this jump is

$$\begin{aligned} C_2 \;=\; & \sqrt{2/3}\sqrt{\Gamma}\Big\{ |g_{-1/2}\rangle_1\ |g_{-1/2}\rangle_2\ {}_1\langle e_{-1/2}|\ {}_2\langle g_{-1/2}| \\ & + |g_{-1/2}\rangle_1\ |g_{+1/2}\rangle_2\ {}_1\langle e_{-1/2}|\ {}_2\langle g_{+1/2}| \\ & + |g_{-1/2}\rangle_1\ |e_{-3/2}\rangle_2\ {}_1\langle e_{-1/2}|\ {}_2\langle e_{-3/2}| \\ & + |g_{-1/2}\rangle_1\ |e_{-1/2}\rangle_2\ {}_1\langle e_{-1/2}|\ {}_2\langle e_{-1/2}| \end{aligned}$$

$$+|g_{-1/2}\rangle_1\ |e_{+1/2}\rangle_2\ {}_1\langle e_{-1/2}|\ {}_2\langle e_{+1/2}|$$
$$+|g_{-1/2}\rangle_1\ |e_{+3/2}\rangle_2\ {}_1\langle e_{-1/2}|\ {}_2\langle e_{+3/2}|\Big\}. \quad (33)$$

Here, the factor $\sqrt{2/3}$ is the Clebsch-Gordan coefficient of the corresponding transition. After applying the jump operator C_j, the wave function is still in a superposition state, but it has collapsed into a subspace of the product state basis vectors, leaving only one ground state level component of the jumped atom populated.

In general, the jump probability into the decay channel j for each of the time-evolution step δt is

$$P_j = \delta t \langle\psi|C_j^\dagger C_j|\psi\rangle. \quad (34)$$

Thus, the jump probability for an example channel 2 in Eq. (33) for each time step is

$$\begin{aligned} P_2 &= \frac{2}{3}\delta t\Gamma\Big\{|\psi_{g_{-1/2}}^{e_{-3/2}}|^2 + |\psi_{g_{+1/2}}^{e_{-3/2}}|^2 + |\psi_{e_{-3/2}}^{e_{-3/2}}|^2 \\ &\quad + |\psi_{e_{-1/2}}^{e_{-3/2}}|^2 + |\psi_{e_{+1/2}}^{e_{-3/2}}|^2 + |\psi_{e_{+3/2}}^{e_{-3/2}}|^2\Big\}. \end{aligned} \quad (35)$$

Paper II presents in detail the implementation of the MCWF method in our lattice studies. There is a large number of numerical problems one has to solve for the MC implementation of two atoms in a lattice. A list of these and their solution is also given in Paper II.

5.3 Red-detuned lattices

In this Section I present the main results from Paper I and Paper II which deal with collision dynamics in red-detuned lattices. The main collision process in this case is radiative heating, see Section 4.1.

Optical lattices, which are detuned a few atomic linewidths below the atomic resonance frequency, provide a very efficient environment for Sisyphus cooling [2]. Once the atoms are localized into the lattice sites, they are still able to move around in the lattice. When the occupation density of the lattice increases one can ask what is the effect of collisions for the Sisyphus cooling dynamics in optical lattices, and how the cold collisions affect the atomic cloud once the atoms are localized.

At the beginning of the efficient cooling period a large fraction of atoms have higher kinetic energy than the optical lattice modulation depth. Atoms then have a high mobility and change their internal state frequently via the

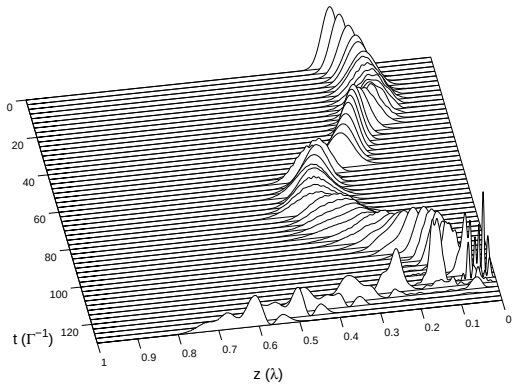

Figure 12: An example of a single wave packet history from the full MC ensemble in position space (note the direction of z-axis because of the viewing angle). At the beginning of the time evolution the atom oscillates in the lattice well which has the center at $z = 0.25\lambda$. It then approaches point $z = 0$ (the position of the fixed atom), collides with another atom, and gains enough kinetic energy to be ejected from the lattice (unpublished).

optical pumping cycles which cool them. *A priori* one might assume that the possible consequence of collisions would be a slowing of the cooling process, heating, and escape of the atoms from the lattice. Radiative heating studies in MOTs show a smooth widening of the momentum probability distribution corresponding to heating for large range of parameters [94,95], see Fig. 8. A similar effect might be expected to occur in an optical lattice as well.

It turns out that the internal structure of the atoms and the spatial dependence of the atom-field coupling changes the consequences of the collisions to some extent. Lattice structure introduces selectivity into the collision processes and atomic dynamics. In a lattice, the mobility of an atom between the lattice sites depends essentially on the kinetic energy, especially once the atoms are localized into the lattice sites. An atom, which has a large oscillation amplitude (corresponding to a large kinetic energy) in the lattice site, has a higher probability to change its internal ground state by optical pumping than an atom which is tightly localized into the vicinity of the center of the potential well[22].

[22]The atomic wave packet here describes a superposition of the populations in the vibrational states of a lattice potential. Thus the wave packet may have rich dynamical

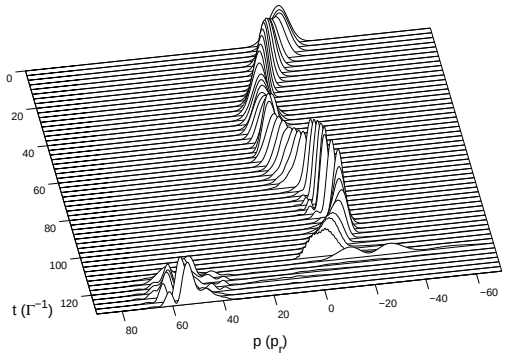

Figure 13: The same MC history as in Fig. 12 but shown here in momentum space. The population is transferred to the high values of momentum due to the collision (unpublished).

Since the high kinetic energy atoms are more mobile compared to their low kinetic energy partners, the high kinetic energy atoms have also a higher collision probability. During the same period of time the high-energy atoms change their internal ground state and the corresponding optical potential more often than tightly localized atoms. Thus, the coverage of various lattice sites, and the corresponding collision probability, is higher for more mobile atoms.

With these assumptions the consequence of collisions might be simple heating of the atomic cloud, or escape of the atoms from the lattice. The essential incredient for a large kinetic energy increase is a high excitation probability of a quasimolecule. This depends on the curvature of the molecular potentials at a resonant Condon point and especially on the relative velocity between the colliding atoms. The optical lattice modulation depth defines the initial velocity distribution of the atoms when they start to move between the lattice sites after localization. It turns out that in a typical lattice, detuned a few atomic linewidths below the atomic resonance, and for lattice depths of a few hundred recoil energies, the surroundings are very favourable for strong excitation of the quasimolecule and the corresponding large kinetic energy changing collisions. The consequence is that the atoms mainly leave the lattice when colliding, and the total effect is the ejection of the hot atoms from the lattice. The ones which remain in a lattice have

features like breathing and oscillations in a single lattice site [108].

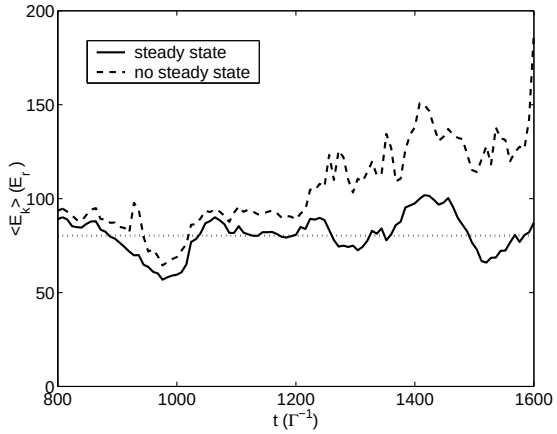

Figure 14: Time evolution of the kinetic energy of the MC ensemble. For critical momentum $p_c = 60\hbar k_r$ (dashed line) the steady state is not reached indicating a too large choice for p_c. Collisions increase the kinetic energy and the collided atoms are out of the recapture range, and thus escape from the lattice. For $p_c = 40\hbar k_r$ (solid line) the steady state is reached and the atoms are recaptured in the lattice. The dotted line indicates the steady state value.

lower average kinetic energy per atom than in the low occupation density case of the lattice when there is no need to account for the interactions between the atoms. Figures 12 and 13 show in position and momentum spaces, respectively, an example of a collision which ejects the atoms from the lattice.

It is a quite subtle point to define which atoms have flown out from the lattice and which remain since it is not possible to give an exact critical velocity. The nature of the cooling optical pumping cycles is stochastic. If the velocity is in the critical range, some of the histories with equal velocities may be recaptured into the lattice while the others escape. The solution for the problem is given by the time evolution of the average kinetic energy per atom, see Fig. 14. If the chosen critical momentum p_c is too high there is no steady state formation (dashed line in Fig. 14). For an appropriate choice of p_c the steady state is still reached (solid line in Fig. 14).

The selective escape mechanism resembles evaporative cooling used to produce BEC in magnetic traps. Here the rethermalization of the remaining atoms is more limited, though. Anyhow, spatial dependence of the laser field introduces selective heating of the hot atoms, and the consequent es-

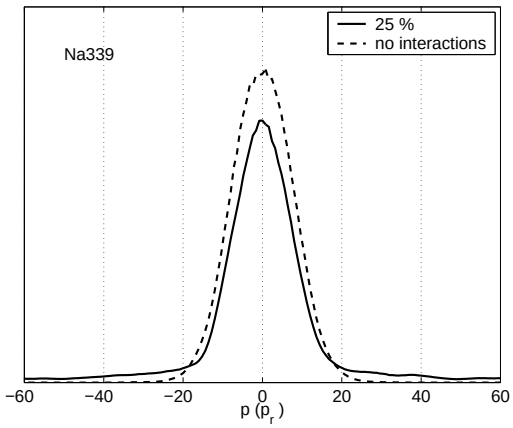

Figure 15: An example of momentum probability distributions for interacting and non–interacting atoms in a red-detuned optical lattice. The momentum p is expressed in the recoil unit $p_r = \hbar k_r$. For interacting atoms the distribution gets narrower compared to non-interacting atoms. The results correspond to a sodium lattice with lattice depth $U_0 = 339E_r$.

cape from the lattice. It would probably be too far reaching to claim that this effect should be visible in an experiment. Our model neglects the reabsorption of photons which may clearly affect the total thermodynamics of the atomic cloud at high densities, and we neglect also the Doppler cooling. Thus we have revealed one important aspect of the thermodynamics of a densely-populated near-resonant optical lattice but the solution for the complete problem is simply out of reach for the modern computational resources.

Figure 15 shows an example of the results for collisions in a red-detuned lattice. This example is for a sodium lattice of depth $U_0 = 339E_r$. The comparison is done between the momentum probability distributions of the interacting and non-interacting cases with occupation density of 25% of the lattice. The central peak is clearly narrower when the interactions between the atoms have been included. This central peak corresponds to the atoms which are trapped in a lattice, and the wide wings correspond to background atoms which are presumably out of the recapture range of the lattice and ejected from the lattice.

One can calculate by semi-classical means the excitation and survival probability for various molecular potentials. We have done a simple semi-classical analysis by using Landau-Zener approach in Paper II. This analysis

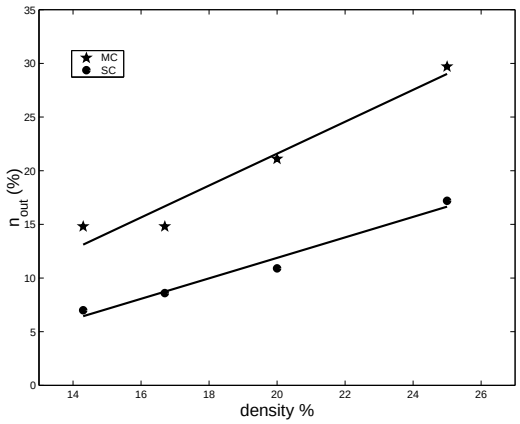

Figure 16: An estimate of the escaped atoms. The percentage of lost atoms as a function of the occupation density of the lattice is shown. MC stands for Monte Carlo and SC for the semiclassical results which take into account only one attractive molecular state. The solid lines are linear fits (unpublished).

supports the conclusions presented above and shows the high probability for the atom pair to gain kinetic energy by the amount with which the collision partners are kicked out from the lattice. Details of the semiclassical analysis can be found in Paper II.

For our selected atomic level structure there exists five different attractive molecular states, see Fig. 11. The semiclassical analysis shows that the potential which becomes resonant first (the one for which the Condon point r_c is the largest) has a dominant role in the heating process. This conclusion is further supported by the results in Fig. 16 (unpublished). This figure shows a comparison of the percentage of lost atoms given by simulation, and by semiclassical analysis which takes into account only the first-resonant potential. The semiclassical result is roughly half of the simulation result suggesting that the first resonant molecular state is responsible already for half of the escaped atoms. The molecular states which are left make a smaller contribution to the heating process.

5.4 Blue-detuned lattices

The prospect of using the trapping and cooling lasers for efficient optical shielding has been studied in Paper III. Complete optical shielding would make collisions between atoms, when they end up in a same lattice, elastic,

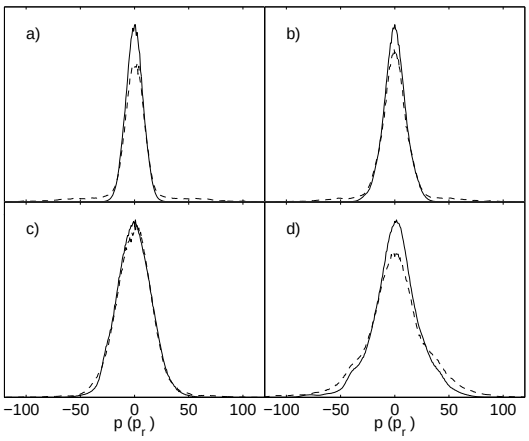

Figure 17: The momentum probability distributions for the $\delta = 5\Gamma$ blue lattice case. The Rabi frequencies are: a) $\Omega = 1.5\Gamma$, b) $\Omega = 2.0\Gamma$, c) $\Omega = 3.0\Gamma$, and d) $\Omega = 5.0\Gamma$. The momentum p is expressed in the recoil unit $p_r = \hbar k_r$. The dashed line is for the interacting and the solid line for the non–interacting atoms. When Ω increases the regime changes from incomplete shielding, a) and b), to complete shielding, c), and finally to off–resonant heating in d). The momentum distributions also get wider due to the deepening of the lattice with increasing Ω.

and it would also prevent atoms from close encounters, preventing, e.g., inelastic hyperfine changing collisions. Thus efficient optical shielding could be beneficial in optical lattices in addition to the typical darkness of the blue-detuned lattices. The number of scattered photons in gray-lattices can be rougly two orders of magnitude smaller than in MOTs [45]. The role of the radiation pressure due to the reabsorption of photons diminishes, and our simplified model describes in a more realistic way the total thermodynamics of the atomic cloud, not only the collision aspect of the thermodynamics.

In our studies we have used the antiparamagnetic regime of the Grynberg-Courtois lattice, with the atomic level structure $J_e = J_g = 1$ shown in Figs. 4 and 5. Rubidium-87 has the corresponding ground and excited state hyperfine components, and in the antiparamagnetic regime the cooling mechanism resembles the traditional Sisyphus cooling.

Figure 17 presents the results of the simulations where the detuning is fixed to $\delta = 5\Gamma$. The results show clearly how the efficiency of the shielding changes. When the coupling laser is weak, a large number of the collisions

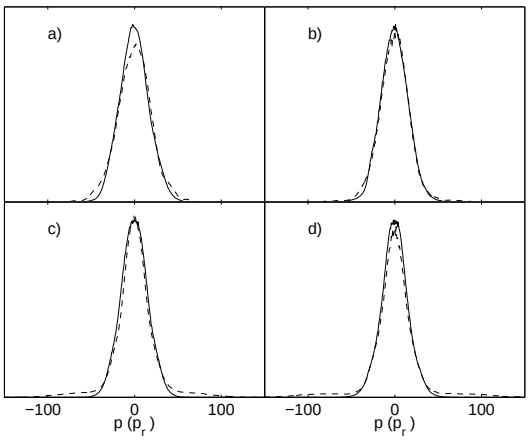

Figure 18: Momentum distributions for fixed $U_0 \sim 710E_r$. a) $\delta = 1.5\Gamma$ b) $\delta = 5.0\Gamma$ c) $\delta = 7.0\Gamma$ d) $\delta = 10.0\Gamma$. The off-resonant processes play a role at the small detuning, a). In the intermediate detuning shielding may become complete and the collisions between atoms are elastic, b). For larger detuning the shielding is incomplete, c) and d).

are still inelastic ones. Wide wings appear in the momentum probability distribution, see Figs. 17 (a) and 17 (b). All the population, which is excited at the Condon point, does not return to the ground state when the atoms move apart again. The quasimolecule slides down on the tail of the repulsive state producing a mild heating effect [25]. For a moderate field strength it is hard to see differencies between the distributions for the interacting and non-interacting atoms, Fig. 17 (c). The optical shielding has become complete and atoms collide elastically when they end up in the same lattice site. The collision partners begin to move apart at large internuclear distances and also the short range unwanted effects are avoided. A further increase in the laser field strength makes it possible for the population to be excited into the attractive molecular state by off-resonant means [96]. This is the reason for the deviation of the two distributions in Fig. 17 (d), where the appearance of the wings is also qualitatively different than in the weak-field case of incomplete shielding.

Figure 18 presents another view to the shielding studies. Instead of keeping the laser detuning fixed, here the lattice modulation depth is kept nearly constant. It turns out that for a very small detuning, Fig. 18 (a), the off-resonant effects heat the atomic cloud. This corresponds to the regime where $\Omega/\delta > 1$, and the steady state formation between the ground and the

excited states surpasses the dynamical resonant excitation process. When the detuning is increased, the point of complete shielding is reached, Fig. 18 (b). In the region where $\Omega/\delta \ll 1$, Fig. 18 (c) and (d), shielding becomes incomplete again due to the weak excitation and stimulated re-excitation in Condon point.

The results demonstrate clearly that the co-existence of cooling, trapping, and shielding processes is possible in blue-detuned near-resonant optical lattices. The shielding process is not always complete but by the careful choice of parameters shielding becomes very efficient. Moreover, this can be obtained within a very typical and convenient parameter regime for near-resonant lattices, e.g., in Fig. 17 (c) $\delta = 5\Gamma$, $\Omega = 3\Gamma$, and $U_0 = 712E_r$. An important benefit of complete shielding is that it can be produced with the same lasers which provide the cooling and trapping. Thus there is no need for additional shielding lasers as in MOTs.

Even though the available occupation densities in near-resonant optical lattices have been very low so far, the metastable rare-gas atoms could provide a convenient case for an experimental study of shielding in optical lattices due to the clear ion signal that marks collision events [109, 110].

The experimental work on optical shielding in MOTs show the saturation of the shielding phenomena when the intensity of the laser field is increased [8]. The saturation has not been present in earlier theoretical studies of shielding [25, 96], and we do not see the saturation of shielding here either. The results presented in Paper III seem to confirm the view that the saturation does not arise due to spontaneous emission effects [25]. The reason for the saturation of shielding is still unclear. It has been attributed to various processes, in addition to the above-mentioned premature termination of shielding via spontaneous emission [25]. Other possibilities include counterintuitive or off-resonant processes involving different partial waves, or other processes that similarly involve multiple states (in contrast to the basic two-state approaches [8,97,111,112]). Anyhow, since our model is limited, we can not conclusively say that saturation of shielding should be absent in a lattice experiment.

So far there has been very few cold collision studies in optical lattices [113, 114]. I hope that our work can serve as a motivation for experimentalists to do shielding studies in blue-detuned optical lattices.

5.5 Collision rates

The results of Papers I and II show that in our selected parameter regime, i.e., the typical parameter regime for near-resonant lattices, the motion

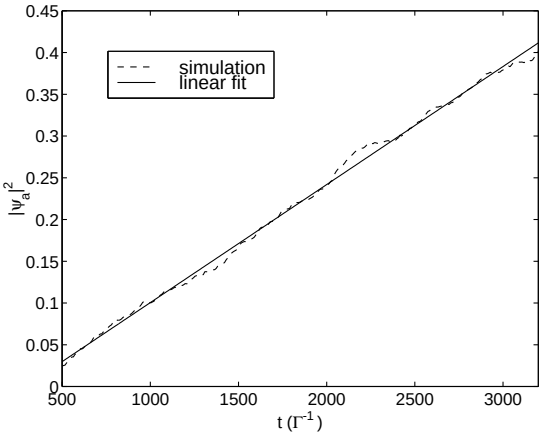

Figure 19: An example ($U_0 = 936E_r$, occupation density $\rho_0 = 20\%$) of the accumulation region population $|\psi_a|^2$ as a function of time. The binary collision rate R is obtained from the slope of the curve β.

of the atom *between* the lattice sites (or in the lattice site occupied by the single atom only) is not strongly affected by other atoms, not at least for the occupation densities which we have used (maximum 25%). Hence, binary interactions between the atoms come into play only when two atoms simultaneously occupy the same lattice site. This makes it possible to develop a method to calculate the average rate at which two atoms end up in the same site, and the consequent cold collision rate in a lattice, by following the trajectories of single atoms[23]. Paper IV presents this type of method. Collision rate describes here the rate of occurrence of radiative heating events in a red-detuned lattice, or optical shielding events, if blue-detuned light is used. It is assumed that the two atoms always collide when they end up in the same lattice site. For the parameters used here, this assumption is confirmed by the results in Papers I and II.

The basic idea of the developed method is simple. It is possible to follow the trajectory of an atom in a single atom MCWF optical lattice simulation. Trajectories in position space can give information about the rate at which atoms travel over the average distance z_a between the atoms, which in turn gives information about the binary collision rate in a lattice[24].

[23]Cold collision rate refers here to the average rate of atoms to reach the region of the resonant Condon point in the presence of near-resonant light.

[24]The average distance between atoms z_a corresponds to the mean free path of atoms between collision events in our one-dimensional model.

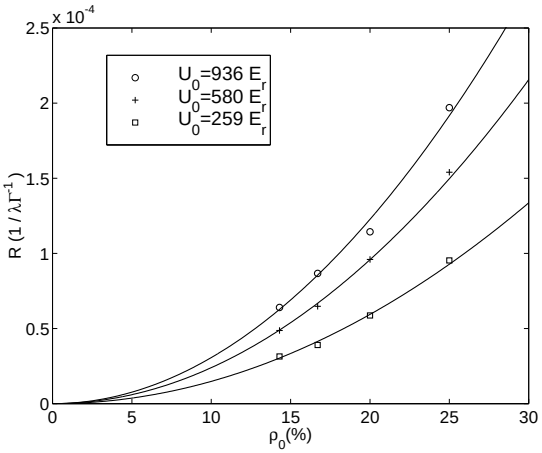

Figure 20: The binary collision rate R for three different lattice depths U_0 as a function of occupation density ρ_0 of the lattice. The points show the simulation results, and the solid lines the quadratic collision rate curves averaged from the simulation results for the specific lattice.

To calculate the collision rate, like presented in Paper IV, we need to know how the atomic population, as a function of time, arrives to the region of space $|z| > z_a$ when the atom is located around the point $z = 0$ at the beginning of the time evolution. In other words, we calculate

$$|\psi_a|^2(t) = \int_{|z|>z_a} \psi^*(z,t)\psi(z,t)dz. \tag{36}$$

Figure 19 shows an example of this. Specifically, it shows how the population accumulates into the area beyond the average distance between the atoms, i.e., into the area $|z| > z_a$ called accumulation region, for a specific case where occupation density of the lattice is 20%[25]. We get the accumulation rate of the population by doing a linear fit to the simulation result and taking the slope β of the accumulation curve. The collision rate per unit time and unit volume (length in our 1D case) is then given by

$$R = \beta/z_a, \tag{37}$$

where z_a is the average distance between the atoms.

[25]To calculate the collision rate correctly, the population flow into the accumulation region has to be made unidirectional. A trick how to do this, see Paper IV.

In Fig. 20 the calculated collision rates as a function of the occupation density of the lattice for three different lattice depths are displayed. In our simple 1D case the collision rate does not depend on the scattering cross section and collisions are a measure of transport in a lattice. This was also the case in the experimental study of Ref. [114]. In both cases the collision rate has a quadratic behaviour.

The points in Fig. 20 are the simulation results and the solid lines quadratic fits. It is interesting to note from the Monte Carlo point of view that we get results for a wide density range by doing simulations for only a very few values of density. The possibility of obtaining the result for all the values of the variable, in this case occupation density, from single Monte Carlo ensembe is a new feature in MCWF simulations to our knowledge, at least when MCWF method is applied to cold collision problems.

Two-atom collision simulations in a lattice described in previous Sections are computationally very heavy. It would be useful to find more simple means to do collision studies in optical lattices. The method presented above presents a step in this direction. For example, if the semiclassical analysis shows that for particular parameter values the colliding atoms have a high probability to be ejected from the lattice due to radiative heating, then the collision rate described here gives directly the loss rate of atoms from the lattice. MCWF simulations for one atom, like the ones reported in Paper IV, are fairly simple and fast to perform. This is especially true when compared to the two-atom case. Thus the combination of these simple one-atom simulations with semiclassical models for intra-well collision effects have a potential to simplify the studies of binary collisions in optical lattices.

6 Conclusions

We have studied the cold collision dynamics between atoms in near-resonant red and blue-detuned optical lattices. The applied methods have been mainly based on the Monte Carlo wave-function method. A semiclassical analysis has been done which supports the conclusions drawn from the full quantum-mechanical calculations.

The implementation of the MCWF method to study cold collisions in optical lattices is not straightforward and the simulations have been very demanding from the computer resource point of view. This is due the internal structure of atoms, coupling to the electromagnetic environment, position dependent coupling of the atoms to the laser field, and position dependent coupling between the atoms.

The results for near-resonant red-detuned lattices are in quite a sharp contrast to the interaction studies in magneto-optical traps. Instead of heating, a cooling due to the selection of collision partners from high kinetic energy atoms is seen in the simulation results. The blue-lattice results clearly show the applicability of optical shielding. Future collision studies require simplifications, for which we propose a simple way to calculate the collision rate in optical lattices.

In the past there has been many studies of cold collisions in magneto-optical traps. The work presented in this thesis extends the regime of cold collision studies into the realm of optical lattices. This is far from being a trivial step. The major reason for this is that for sub-Doppler cooling mechanisms, which exploit various polarization states of a laser field, it is necessary to account for the internal structure of atoms, and this greatly complicates the total system under study and the calculations done. Moreover, it is not enough to formulate the problem using only the relative motion between the atoms in a constant laser field. The position of the atoms with respect to a lattice structure has to be accounted also.

We have shown that it is meaningful to study cold collisions in optical lattices, even within the limits of our simple model, whose implementation of the solution is far from being simple. Our lattice calculations present a step forward in the understanding of the physics of atoms in near-resonant optical lattices.

Appendices

A Numerical methods

Since the method we have used is based on the MCWF simulations, the essential incredient in the solution is the time propagation of the system wave-function. In other words, finding the solution for the time dependent Schrödinger equation

$$i\hbar\frac{\partial|\psi\rangle}{\partial t} = H|\psi\rangle. \tag{38}$$

Formally solving this equation over time step δt gives

$$|\psi(t_0+\delta t)\rangle = U|\psi(t_0)\rangle, \tag{39}$$

where the time evolution operator U reads

$$U = \exp\left(-\frac{iH\delta t}{\hbar}\right). \tag{40}$$

The time evolution operator U, which includes the Hamiltonian H, can be split into three parts as

$$H = H_V + H_K + H_D. \tag{41}$$

When H is in matrix form, H_V has an off-diagonal part, which in our case accounts for the atom-field coupling and the interaction between the atoms, H_K is the diagonal kinetic part, and H_D includes the non-kinetic diagonal part, i.e., decay and detuning.

For non-commuting operators A and B we can write to second order accuracy [108]

$$\exp(A+B) \simeq \exp(A/2)\exp(B)\exp(A/2). \tag{42}$$

It is important to note that the Hamiltonian H does not have any explicit time dependence in our case, and as we take many consecutive time steps during the evolution, we finally approximate the wave function at time $t_0 + n\delta t$ by

$$|\psi(z, t_0+n\delta t)\rangle \simeq \left[\prod_{k=0}^{n-1} U_V U_D^{1/2} U_K U_D^{1/2}\right]|\psi(z,t_0)\rangle. \tag{43}$$

Here,

$$U_D = \exp(-iH_D\delta t/\hbar) \tag{44}$$

and

$$U_K = \mathcal{F}^{-1} \exp(-i\delta t \frac{\hbar k^2}{2M}) \mathcal{F} \tag{45}$$

where $\mathcal{F}$ and $\mathcal{F}^{-1}$ denote the Fourier and inverse Fourier transforms. Finally, U_V can be written as

$$U_V = S \exp(D) S^{-1}, \tag{46}$$

where S contains the eigenvectors and D the eigenvalues of H_V. U_V corresponds now to a change of basis, multiplication by exponentials of eigenvalues, and a change of basis back to the product state basis. The above form for the temporal evolution of $|\psi\rangle$ is quite straightforward to implement and fast on a computer, e.g., 20% faster than the Crank–Nicholson method [108]. The difference in the speed of the two methods is not very large but still plays an essential role since the simulations done are at the edge of the available computer capacity and CPU time. The relative speed of the Fourier and Crank-Nicholson method may vary depending on the system under study, computers used and available sub-routine libraries. We have performed the simulations in Silicon Graphics computers and it seems that the Fourier transformation routines have been well optimized in the Silicon Graphics subroutine library for a good performance of the computer.

B Required computational resources

The numerical simulations are demanding since we are dealing with a 36 level quantum system[26] including various position dependent couplings and dissipative coupling to the environment. We use 32 processors of an SGI Origin 2000 machine, which has 128 MIPS R12000 processors of 1 GB memory per processor [27]. The total memory taken by a single simulation (fixed δ, Ω, occupation density ρ_o, and atomic species) is 14 GB, and generating a single history requires 6 hours of CPU time in red-detuned lattice studies. A simulation of 128 ensemble members then requires a total CPU time which is roughly equal to one month. The normal clock time is, of course, much shorter (roughly 22 hours) since we take advantage of powerful parallel processing for which the MCWF simulations suit very well[28].

[26] For a blue-detuned case, the number of levels in the two-atom simulations can be reduced to 9, see Section 3.2.1.

[27] See CSC, the Finnish IT center for science, webpage www.csc.fi for details.

[28] The communication between the processors occurs mainly at the beginning and at the end of the simulation. From a parallel programming point of view, this type of problems are sometimes referred in the literature as "embarrassingly" parallel problems.

References

[1] E. F. Nichols and G. F. Hull, *A Preliminary Communication on the Pressure of Heat and Light Radiation*, Phys. Rev. **13**, 307 (1901).

[2] J. Dalibard and C. Cohen-Tannoudji, *Laser Cooling below the Doppler Limit by Polarization Gradients: Simple Theoretical Models*, J. Opt. Soc. Am. B **6**, 2023 (1989).

[3] P. S. Jessen and I. H. Deutsch, *Optical Lattices*, Adv. At. Mol. Opt. Phys. **37**, 95 (1996).

[4] D. R. Meacher, *Optical Lattices - Crystalline Structures Bound by Light*, Contemp. Phys. **39**, 329 (1998).

[5] S. Rolston, *Optical Lattices*, Phys. World **11** (10), 27 (1998).

[6] L. Guidoni and P .Verkerk, *Optical Lattices: Cold Atoms Ordered by Light*, J. Opt. B **1**, R23 (1999).

[7] K.-A. Suominen, *Theories for Cold Atomic Collisions in Light Fields*, J. Phys. B **29**, 5981 (1996).

[8] J. Weiner, V. S. Bagnato, S. Zilio, and P. S. Julienne, *Experiments and Theory in Cold and Ultracold Collisions*, Rev. Mod. Phys. **71**, 1 (1999).

[9] H. J. Metcalf and P. van der Straten, *Laser Cooling and Trapping* (Springer, New-York, 1999).

[10] C. S. Adams and E. Riis, *Laser Cooling and Trapping of Neutral Atoms*, Prog. Quant. Electr. **21**, 1 (1997).

[11] F. Dalfovo, S. Giorgini, L. P. Pitaevskii, and S. Stringari, *Theory of Bose-Einstein Condensation in Trapped Gases*, Rev. Mod. Phys. **71**, 463 (1999).

[12] A. J. Leggett, *Bose-Einstein Condensation in the Alkali Gases: Some Fundamental Concepts*, Rev. Mod. Phys. **73**, 307 (2001).

[13] C. Cohen-Tannoudji, in *Les Houches, Session LIII, 1990 - Fundamental Systems in Quantum optics*, edited by J. Dalibard, J.-M. Raimond, and J. Zinn-Justin (Elsevier Science Publishers B.V., Amsterdam, 1992), p. 1.

[14] C. Cohen-Tannoudji, in *Proceedings of the International School of Physics Enrico Fermi, Course CXVIII - Laser Manipulation of Atoms and Ions*, edited by E. Arimondo, W. D. Phillips, and F. Strumia (Elsevier Science Publishers B.V., Amsterdam, 1994), p. 99.

[15] G. Grynberg and C. Triché, in *Proceedings of the International School of Physics Enrico Fermi, Course CXXXI - Coherent and Collective Interactions of Particles and Radiation Beams*, edited by A. Aspect, W. Barletta, and R. Bonifacio (IOS Press, Amsterdam, 1996), p. 243.

[16] A. Hemmerich, M. Weidemüller, and T. W. Hänsch, in *Proceedings of the International School of Physics Enrico Fermi, Course CXXXI - Coherent and Collective Interactions of Particles and Radiation Beams*, edited by A. Aspect, W. Barletta, and R. Bonifacio (IOS Press, Amsterdam, 1996), p. 503.

[17] K. Burnett, P. Julienne, P. Lett, and K.-A. Suominen, *Cold Atoms See the Light*, Phys. World **8** (10), 42 (1995).

[18] S. Chu, J. E. Bjorkholm, A. Ashkin, and A. Cable, *Experimental Observation of Optically Trapped Atoms*, Phys. Rev. Lett. **57**, 314 (1986).

[19] S. Stenholm, *The Semiclassical Theory of Laser Cooling*, Rev. Mod. Phys. **58**, 699 (1986).

[20] P. Lett, R. Watts, C. Westbrook, W. Phillips, P. Gould, and H. Metcalf, *Observation of Atoms Laser Cooled below the Doppler Limit*, Phys. Rev. Lett. **61**, 169 (1988).

[21] M. Machholm, P. S. Julienne, and K.-A. Suominen, *Calculations of Collisions Between Cold Alkaline-Earth-Metal Atoms in a Weak Laser Field*, Phys. Rev. A **64**, 033425 (2001).

[22] P. J. Ungar, D. S. Weiss, E. Riis, and S. Chu, *Optical Molasses and Multilevel Atoms: Theory*, J. Opt. Soc. Am. B **6**, 2058 (1989).

[23] A. Aspect, E. Arimondo, R. Kaiser, N. Vansteenkiste, and C. Cohen-Tannoudji, *Laser Cooling below the One-Photon Recoil Energy by Velocity-Selective Coherent Population Trapping*, Phys. Rev. Lett. **61**, 826 (1988).

[24] L. Marcassa, S. Muniz, E. de Queiroz, S. Zilio, V. Bagnato, J. Weiner, P. S. Julienne, and K.-A. Suominen, *Optical Suppression of Photoassociative Ionization in a Magneto-Optical Trap*, Phys. Rev. Lett. **73**, 1911 (1994).

[25] K.-A. Suominen, M. J. Holland, K. Burnett, and P. S. Julienne, *Optical Shielding of Cold Collisions*, Phys. Rev. A **51**, 1446 (1995).

[26] J. L. Roberts, N. R. Claussen, S. L. Cornish, and C. E. Wieman, *Magnetic Field Dependence of Ultracold Inelastic Collisions Near a Feshbach Resonance*, Phys. Rev. Lett. **85**, 728 (2000).

[27] F. K. Fatemi, K. M. Jones, and P. D. Lett, *Observation of Optically Induced Feshbach Resonances in Collisions of Cold Atoms*, Phys. Rev. Lett. **85**, 4462 (2000).

[28] M. D. Barrett, J. A. Sauer, and M. S. Chapman, *All-Optical Formation of an Atomic Bose-Einstein Condensate*, Phys. Rev. Lett. **87**, 010404 (2001).

[29] C. Orzel, A. K. Tuchman, M. L. Fenselau, M. Yasuda, and M. A. Kasevich, *Squeezed States in a Bose-Einstein Condensate*, Science **291**, 2386 (2001).

[30] G. Birkl, M. Gatzke, I. H. Deutsch, S. L. Rolston, and W. D. Phillips, *Bragg Scattering from Atoms in Optical Lattices*, Phys. Rev. Lett. **75**, 2823 (1995).

[31] M. Weidemüller, A. Hemmerich, A. Görlitz, T. Esslinger, and T. W. Hänsch, *Bragg Diffraction in an Atomic Lattice Bound by Light*, Phys. Rev. Lett. **75**, 4583 (1995).

[32] M. Ben Dahan, E. Peik, Y. Castin, and C. Salomon, *Bloch Oscillations of Atoms in an Optical Potential*, Phys. Rev. Lett. **76**, 4508 (1996).

[33] S. R. Wilkinson, C. F. Bharucha, K. W. Madison, Q. Niu, and M. G. Raizen, *Observation of Atomic Wannier-Stark Ladders in an Accelerating Optical Potential*, Phys. Rev. Lett. **76**, 4512 (1996).

[34] M. C. Fischer, B. Gutiérrez-Medina, and M. G. Raizen, *Observation of the Quantum Zeno and Anti-Zeno Effects in an Unstable System*, Phys. Rev. Lett. **87**, 040402 (2001).

[35] W. K. Hensinger, H. Häffner, A. Browaeys, N. R. Heckenberg, K. Helmerson, C. McKenzie, G. J. Milburn, W. D. Phillips, S. L. Rolston, H. Rubinsztein-Dunlop, and B. Upcroft, *Dynamical Tunneling of Ultracold Atoms*, Nature **412**, 52 (2001).

[36] V. L. Letokhov, *Narrowing of the Doppler Width in a Standing Light Wave*, JETP Lett. **7**, 272 (1968).

[37] M. M. Burns, J.-M. Fournier, and J. A. Golovchenko, *Optical Matter: Crystallization and Binding in Intense Optical Fields*, Science **249**, 749 (1990).

[38] Y. Castin, J. Dalibard, and C. Cohen-Tannoudji, in *Proceedings of Light Induced Kinetic Effects on Atoms, Ion and Molecules*, edited by L. Moi, S. Gozzini, C. Gabbanini, E. Arimondo, and F. Strumia (ETS Editrice, Pisa, 1991), p. 1.

[39] C. Mennerat-Robilliard, L. Guidoni, J.-Y. Courtois, and G. Grynberg, *Cooling and Trapping Cesium Atoms in π-Polarized Potential Wells: The Jumping Regime of Optical Lattices*, Europhys. Lett. **38**, 429 (1997).

[40] M. S. Shahriar, P. R. Hemmer, M. G. Prentiss, P. Marte, J. Mervis, D. P. Katz, N. P. Bigelow, and T. Cai, *Continuous Polarization-Gradient Precooling-Assisted Velocity-Selective Coherent Population Trapping*, Phys. Rev. A **48**, R4035 (1993).

[41] P. Marte, R. Dum, R. Taïeb, P. Zoller, M. S. Shahriar, and M. Prentiss, *Polarization-Gradient-Assisted Subrecoil Cooling: Quantum Calculations in One Dimension*, Phys. Rev. A **49**, 4826 (1994).

[42] J. Guo and P. R. Berman, *One-Dimensional Laser Cooling with Linearly Polarized Fields*, Phys. Rev. A **48**, 3225 (1993).

[43] M. Weidemüller, T. Esslinger, M. A. Ol'Shanii, A. Hemmerich, and T. Hänsch, *A Novel Scheme for Efficient Cooling below the Photon Recoil Limit*, Europhys. Lett. **27**, 109 (1994).

[44] J. Guo and J. Cooper, *Probe-Transmission Spectrum of a Blue-Detuned Optical Lattice*, Phys. Rev. A **52**, R1819 (1995).

[45] A. Hemmerich, M. Weidemüller, T. Esslinger, C. Zimmermann, and T. Hänsch, *Trapping Atoms in a Dark Optical Lattice*, Phys. Rev. Lett. **75**, 37 (1995).

[46] G. Grynberg and J.-Y. Courtois, *Proposal for a Magneto-Optical Lattice for Trapping atoms in Nearly-Dark States*, Europhys. Lett. **27**, 41 (1994).

[47] H. Stecher, H. Ritsch, P. Zoller, F. Sander, T. Esslinger, and T. W. Hänsch, *All-Optical Gray Lattice For Atoms*, Phys. Rev. A **55**, 545 (1997).

[48] K. I. Petsas, J.-Y. Courtois, and G. Grynberg, *Temperature and Magnetism of Gray Optical Lattices*, Phys. Rev. A **53**, 2533 (1996).

[49] C. J. Hood, T. W. Lynn, A. C. Doherty, A. S. Parkins, and H. J. Kimble, *The Atom-Cavity Microscope: Single Atoms Bound in Orbit by Single Photons*, Science **287**, 1447 (2000).

[50] J. I. Kim, R. B. B. Santos, and P. Nussenzveig, *Manipulation of Cold Atomic Collisions by Cavity QED Effects*, Phys. Rev. Lett. **86**, 1474 (2001).

[51] J. Dalibard, Y. Castin, and K. Mølmer, *Wave-Function Approach to Dissipative Processes in Quantum Optics*, Phys. Rev. Lett. **68**, 580 (1992).

[52] K. Mølmer, Y. Castin, and J. Dalibard, *Monte Carlo Wave-Function Method in Quantum Optics*, J. Opt. Soc. Am. B **524**, 524 (1993).

[53] K. Mølmer and Y. Castin, *Monte Carlo Wavefunctions in Quantum Optics*, Quantum Semiclass. Opt. **8**, 49 (1996).

[54] M. B. Plenio and P. L. Knight, *The Quantum-Jump Approach to Dissipative Dynamics in Quantum Optics*, Rev. Mod. Phys. **70**, 101 (1998).

[55] Y. Castin and J. Dalibard, *Quantization of Atomic Motion in Optical Molasses*, Europhys. Lett. **14**, 761 (1991).

[56] P. Marte, R. Dum, R. Taïeb, P. D. Lett, and P. Zoller, *Quantum Wave Function Simulation of the Resonance Fluorescence Spectrum from One-Dimensional Optical Molasses*, Phys. Rev. Lett. **71**, 1335 (1993).

[57] Y. Castin and K. Mølmer, *Monte Carlo Wave-Function Analysis of 3D Optical Molasses*, Phys. Rev. Lett. **74**, 3772 (1995).

[58] F. Intravaia, S. Maniscalco, J. Piilo, and A. Messina, *Quantum Theory of Heating of a Single Trapped Ion*, quant-ph/0206152 .

[59] S. C. Badescu, S. C. Ying, and T. Ala-Nissilä, *Quantum Diffusion of H/Ni(111) through a Monte Carlo Wave Function Formalism*, Phys. Rev. Lett. **86**, 5092 (2001).

[60] K. Berg-Sørensen, Y. Castin, K. Mølmer, and J. Dalibard, *Cooling and Tunneling of Atoms in a 2D Laser Field*, Europhys. Lett. **22**, 663 (1993).

[61] K.-A. Suominen, Y. B. Band, I. Tuvi, K. Burnett, and P. S. Julienne, *Quantum and Semiclassical Calculations of Cold Atom Collisions in Light Fields*, Phys. Rev. A **57**, 3724 (1998).

[62] K. I. Petsas, G. Grynberg, and J.-Y. Courtois, *Semiclassical Monte Carlo Approaches for Realistic Atoms in Optical Lattices*, Eur. Phys. J. D **6**, 29 (1999).

[63] W. Greenwood, P. Pax, and P. Meystre, *Atomic Transport on One-Dimensional Optical Lattices*, Phys. Rev. A **56**, 2109 (1997).

[64] K. I. Petsas, A. B. Coates, and G. Grynberg, *Crystallography of Optical Lattices*, Phys. Rev. A **50**, 5173 (1994).

[65] A. Hemmerich and T. W. Hänsch, *Two-Dimensional Atomic Crystal Bound by Light*, Phys. Rev. Lett. **70**, 410 (1993).

[66] L. Guidoni, C. Triché, P. Verkerk, and G. Grynberg, *Quasiperiodic Optical Lattices*, Phys. Rev. Lett. **79**, 3363 (1997).

[67] A. Sørensen and K. Mølmer, *Spin-Spin Interaction and Spin Squeezing in an Optical Lattice*, Phys. Rev. Lett. **83**, 2274 (1999).

[68] S. Kuhr, W. Alt, D. Schrader, M. Müller, V. Gomer, and D. Meschede, *Deterministic Delivery of a Single Atom*, Science **293**, 278 (2001).

[69] M. T. DePue, C. McCormick, S. L. Winoto, S. Oliver, and D. S. Weis, *Unity Occupation of Sites in a 3D Optical Lattice*, Phys. Rev. Lett. **82**, 2262 (1999).

[70] A. J. Kerman, V. Vuletić, C. Chin, and S. Chu, *Beyond Optical Molasses: 3D Raman Sideband Cooling of Atomic Cesium to High Phase-Space Density*, Phys. Rev. Lett. **84**, 439 (2000).

[71] K. Berg-Sørensen and K. Mølmer, *Bose-Einstein Condensates in Spatially Periodic Potentials*, Phys. Rev. A **58**, 1480 (1998).

[72] D. Jaksch, C. Bruder, J. I. Cirac, C. W. Gardiner, and P. Zoller, *Cold Bosonic Atoms in Optical Lattices*, Phys. Rev. Lett. **81**, 3108 (1998).

[73] D.-I. Choi and Q. Niu, *Bose-Einstein Condensates in an Optical Lattice*, Phys. Rev. Lett. **82**, 2022 (1999).

[74] S. Burger, F. S. Cataliotti, C. Fort, F. Minardi, M. Inguscio, M. L. Chiofalo, and M. P. Tosi, *Superfluid and Dissipative Dynamics of a Bose-Einstein Condensate in a Periodic Optical Potential*, Phys. Rev. Lett. **86**, 4447 (2001).

[75] O. Morsch, J. H. Müller, M. Cristiani, D. Ciampini, and E. Arimondo, *Bloch Oscillations and Mean-Field Effects of Bose-Einstein Condensates in 1D Optical Lattices*, Phys. Rev. Lett. **87**, 140402 (2001).

[76] P. Pedri, L. Pitaevskii, S. Stringari, C. Fort, S. Burger, F. S. Cataliotti, P. Maddaloni, F. Minardi, and M. Inguscio, *Expansion of a Coherent Array of Bose-Einstein Condensates*, Phys. Rev. Lett. **87**, 220401 (2001).

[77] B. Wu and Q. Niu, *Dynamical or Landau Instability?* Comment on Ref. [74], Phys. Rev. Lett. **89**, 08890 (2002).

[78] S. Burger, F. S. Cataliotti, C. Fort, F. Minardi, M. Inguscio, M. L. Chiofalo, and M. P. Tosi, Reply to comment [77], Phys. Rev. Lett. **89**, 088902 (2002).

[79] M. Greiner, O. Mandel, T. Esslinger, T. W. Hänsch, and I. Bloch, *Quantum Phase Transition from a Superfluid to a Mott Insulator in a Gas of Ultracold Atoms*, Nature **415**, 39 (2002).

[80] G. K. Brennen, C. M. Caves, P. S. Jessen, and I. H. Deutsch, *Quantum Logic Gates in Optical Lattices*, Phys. Rev. Lett. **82**, 1060 (1999).

[81] D. Jaksch, H.-J. Briegel, J. I. Cirac, C. W. Gardiner, and P. Zoller, *Entanglement of Atoms via Cold Controlled Collisions*, Phys. Rev. Lett. **82**, 1975 (1999).

[82] P. D. Drummond, K. V. Kheruntsyan, and H. He, *Coherent Molecular Solitons in Bose-Einstein Condensates*, Phys. Rev. Lett. **81**, 3055 (1998).

[83] J. Javanainen and M. Mackie, *Coherent Photoassociation of a Bose-Einstein Condensate*, Phys. Rev. A **59**, R3186 (1999).

[84] D. Jaksch, V. Venturi, J. I. Cirac, C. J. Williams, and P. Zoller, *Creation of a Molecular Condensate by Dynamically Melting a Mott Insulator*, Phys. Rev. Lett. **89**, 040402 (2002).

[85] M. Ol'shanii and D. Weiss, *Producing Bose-Einstein Condensates Using Optical Lattices*, Phys. Rev. Lett. **89**, 090404 (2002).

[86] W. Hofstetter, J.I. Cirac, P. Zoller, E. Demler, and M.D. Lukin, *High-Temperature Superfluidity of Fermionic Atoms in Optical Lattices*, Phys. Rev. Lett. **89**, 220407 (2002).

[87] J. Ruostekoski, G. V. Dunne, and J. Javanainen, *Particle Number Fractionalization of an Atomic Fermi-Dirac Gas in an Optical Lattice*, Phys. Rev. Lett. **88**, 180401 (2002).

[88] N. V. Morrow, S. K. Dutta, and G. Raithel, *Feedback Control of Atomic Motion in an Optical Lattice*, Phys. Rev. Lett. **88**, 093003 (2002).

[89] P. W. Atkins and R. S. Friedman, *Molecular Quantum Mechanics, 3rd edition* (Oxford University Press, Oxford, 1997).

[90] M. Movre and G. Pichler, *Resonance Interaction and Self-Broadening of Alkali Resonance Lines I. Adiabatic Potential Curves*, J. Phys. B **10**, 2631 (1977).

[91] P. S. Julienne and J. Vigué, *Cold Collisions of Ground- and Excited-State Alkali-Metal Atoms*, Phys. Rev. A **44**, 4464 (1991).

[92] R. Wynar, R. S. Freeland, D. J. Han, C. Ryu, and D. J. Heinzen, *Molecules in a Bose-Einstein Condensate*, Science **287**, 1016 (2000).

[93] M. Koštrun, M. Mackie, R. Côté, and J. Javanainen, *Theory of Coherent Photoassociation of a Bose-Einstein condensate*, Phys. Rev. A **62**, 063616 (2000).

[94] M. J. Holland, K.-A. Suominen, and K. Burnett, *Quantal Treatment of Cold Collisions in a Laser Field*, Phys. Rev. Lett. **72**, 2367 (1994).

[95] M. J. Holland, K.-A. Suominen, and K. Burnett, *Cold Collisions in a Laser Field: Quantum Monte Carlo Treatment of Radiative Heating*, Phys. Rev. A **50**, 1513 (1994).

[96] K.-A. Suominen, K. Burnett, and P. S. Julienne, *Role of Off-Resonant Excitation in Cold Collisions in a Strong Field*, Phys. Rev. A **53**, R1120 (1996).

[97] K.-A. Suominen, K. Burnett, P. S. Julienne, M. Walhout, U. Sterr, C. Orzel, M. Hoogerland, and S. L. Rolston, *Ultracold Collisions and Optical Shielding in Metastable Xenon*, Phys. Rev. A **53**, 1678 (1996).

[98] C. Cohen-Tannoudji, B. Diu, and F. Laloë, *Quantum Mechanics,* Vol. I (Wiley-Interscience, Paris, 1977).

[99] E. V. Goldstein, P. Pax, and P. Meystre, *Dipole-Dipole Interaction in Three-Dimensional Optical Lattices*, Phys. Rev. A **53**, 2604 (1996).

[100] C. Boisseau and J. Vigué, *Laser-Dressed Molecular Interactions at Long Range*, Opt. Commun. **127**, 251 (1996).

[101] A. M. Guzmán and P. Meystre, *Dynamical Effects of the Dipole-Dipole Interaction in Three-Dimensional Optical Lattices*, Phys. Rev. A **57**, 1139 (1998).

[102] C. Menotti and H. Ritsch, *Mean-Field Approach to Dipole-Dipole Interaction in an Optical Lattice*, Phys. Rev. A **60**, R2653 (1999).

[103] C. Menotti and H. Ritsch, *Laser Cooling of Atoms in Optical Lattices Including Quantum Statistics and Dipole-Dipole Interactions*, Appl. Phys. B **69**, 311 (1999).

[104] G. W. King and J. H. van Vleck, *Dipole-Dipole Resonance Forces*, Phys. Rev. **55**, 1165 (1939).

[105] H. B. G. Casimir and D. Polder, *The Influence of Retardation on the London-van der Waals Forces*, Phys. Rev. **73**, 360 (1948).

[106] G. Lenz and P. Meystre, *Resonance Fluorescence From Two Identical Atoms In a Standing-Wave Field*, Phys. Rev. A **48**, 3365 (1993).

[107] P. R. Berman, *Resonant Interaction Between Identical Atoms Including Recoil*, Phys. Rev. A **55**, 4466 (1997).

[108] B. M. Garraway and K.-A. Suominen, *Wave Packet Dynamics: New Physics and Chemistry in Femto-Time*, Rep. Prog. Phys. **58**, 365 (1995).

[109] H. Katori and F. Shimizu, *Laser-Induced Ionizing Collisions of Ultracold Krypton Gas in the* $1s_5$ *Metastable State*, Phys. Rev. Lett. **73**, 2555 (1994).

[110] M. Walhout, U. Sterr, C. Orzel, M. Hoogerland, and S. L. Rolston, *Optical Control of Ultracold Collisions in Metastable Xenon*, Phys. Rev. Lett. **74**, 506 (1995).

[111] V. A. Yurovsky and A. Ben-Reuven, *Incomplete Optical Shielding in Cold Atom Traps: Three-Dimensional Landau-Zener Theory*, Phys. Rev. A **55**, 3772 (1997).

[112] R. Napolitano, J. Weiner, and P. S. Julienne, *Theory of Optical Suppression of Ultracold-Collision Rates by Polarized Light*, Phys. Rev. A **55**, 1191 (1997).

[113] H. Kunugita, T. Ido, and F. Shimizu, *Ionizing Collisional Rate of Metastable Rare-Gas Atoms in an Optical Lattice*, Phys. Rev. Lett. **79**, 621 (1997).

[114] J. Lawall, C. Orzel, and S. L. Rolston, *Suppression and Enhancement of Collisions in Optical Lattices*, Phys. Rev. Lett. **80**, 480 (1998).